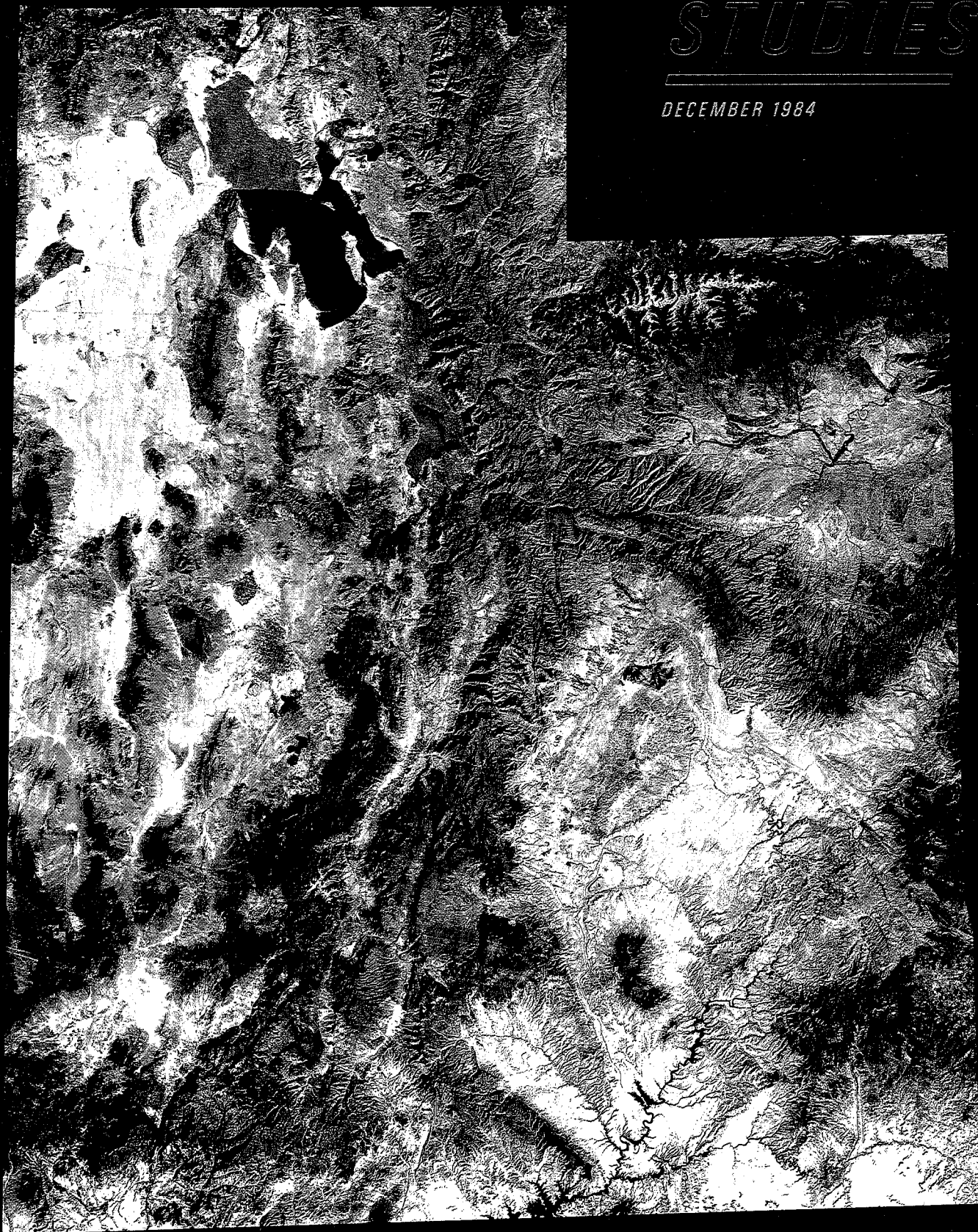


BRIGHAM
YOUNG
UNIVERSITY

GEOLOGY

STUDIES

DECEMBER 1984



VOLUME 31, PART 1

BRIGHAM YOUNG UNIVERSITY GEOLOGY STUDIES

VOLUME 31, PART 1

CONTENTS

Geology of the Northern Canyon Range, Millard and Juab Counties, Utah	John C. Holladay	1
Depositional Environment of the Iron Springs Formation, Gunlock, Utah	Brad T Johnson	29
Shnabkaib Member of the Moenkopi Formation: Depositional Environment and Stratigraphy near Virgin, Washington County, Utah	Ralph E. Lambert	47
Geology of the Mount Ellen Quadrangle, Henry Mountains, Garfield County, Utah	Loren B. Morton	67
Depositional Environments and Paleoecology of Two Quarry Sites in the Middle Cambrian Marjum and Wheeler Formations, House Range, Utah	John C. Rogers	97
Carbonate Petrology and Depositional Environments of Carbonate Buildups in the Devonian Guilmette Formation near White Horse Pass, Elko County, Nevada	Stephen M. Smith	117
Geology of the Steele Butte Quadrangle, Garfield County, Utah	William W. Whitlock	141
Petrography and Microfacies of the Devonian Guilmette Formation in the Pequop Mountains, Elko County, Nevada	Winston L. Williams	167
<hr/>		
A Geologic Analysis of a Part of Northeastern Utah Using ERTS Multispectral Imagery	Robert Brigham Young	187
Publications and Maps of the Department of Geology		213



A publication of the
Department of Geology
Brigham Young University
Provo, Utah 84602

Editors

W. Kenneth Hamblin
Karen Seely

Brigham Young University Geology Studies is published by the Department of Geology. This publication consists of graduate student and faculty research within the department as well as papers submitted by outside contributors. Each article submitted by BYU faculty and outside contributors is externally reviewed by at least two qualified persons.

Cover: LANDSAT Mosaic of the State of Utah. Fall 1976.
U.S. Department of Agriculture, Agricultural Stabilization
and Conservation Service. Salt Lake City, Utah: Aerial
Photography Field Office.

ISSN 0068-1016
Distributed December 1984
12-84 600 74358

CONTENTS

Geology of the Northern Canyon Range, Millard and Juab Counties, Utah, by John C. Holladay	1	Syncline axis thrust	19
Abstract	1	Folds	19
Introduction	1	Canyon Range syncline	19
Location and accessibility	2	Canyon Range anticline	20
Field and laboratory methods	2	Tertiary folds	20
Previous work	3	Normal faults	21
Stratigraphy	3	Bridge Canyon fault	21
Precambrian System	3	Dry Fork fault	21
Pocatello Formation	5	Wide Canyon-east border fault	21
Lower shale member	5	Recent faults	21
Middle quartzite member	5	Tear faults	22
Upper shale and siltstone member	5	Limekiln Canyon fault	22
Blackrock Canyon Limestone	7	Syncline axis fault	22
Caddy Canyon Quartzite	7	Cow Canyon fault	23
Inkom Formation	7	Pavant allochthon	23
Mutual Formation	7	Correlation with exposures in the Pavant	
Lower member	8	Mountains	23
Upper member	8	Canyon Range thrust footwall ramp	23
Cambrian System	8	Structural evolution of the Canyon Range	24
Cambrian System—Canyon Range allochthon	9	Overview	24
Tintic Quartzite	9	Directions of thrust movements	25
Pioche Formation	9	Magnitudes of thrust displacement	25
Howell Limestone	10	Leamington Canyon fault	25
Chisholm Formation	10	Salt tectonism	26
Dome Limestone	10	Economic geology	26
Whirlwind Formation	10	Conclusions	27
Swasey Limestone	10	Acknowledgments	27
Wheeler Shale	10	References cited	27
Undivided Cambrian carbonates	10	Figures	
Cambrian System—Pavant allochthon	11	1. Index map of northern Canyon Range	2
Tintic Quartzite	11	2. Stratigraphic column of Canyon Range alloch-	
Pioche Formation (?)	11	thon	4
Undivided Cambrian carbonates	11	3. Stratigraphic column of Pavant allochthon	5
Ordovician System	11	4. Outcrop of middle member of Pocatello Forma-	
Pogonip Group	11	tion	6
Cretaceous and Tertiary Systems	11	5. Precambrian facies cross section	6
Canyon Range Formation	13	6. Outcrop of upper member of Pocatello Forma-	
Lower member	13	tion	7
Middle member	13	7. Outcrop of Blackrock Canyon Limestone	8
Upper member	15	8. Geological map of northern Canyon Range in pocket	
Red beds of Wide Canyon	15	9. Strike valley eroded along Inkom Formation	9
Fool Creek Conglomerate	15	10. Middle Cambrian stratigraphy of Canyon	
Oak City Formation	15	Range and Pavant allochthons	12
Quaternary System	16	11. Topographic profile of middle member of Can-	
Structural geology	16	yon Range Formation	14
Thrust faults	16	12. Canyon Range Formation folded in syncline	
Canyon Range thrust fault (eastern exposure) ..	16	axis	14
Canyon Range thrust fault (western exposure) ..	16	13. Structural evolution of Canyon Range	17
Canyon Range thrust fault east of Oak City	16	14. Eastern exposure of Canyon Range klippe	18
		15. Western exposure of Canyon Range klippe	18

16. Canyon Range thrust east of Oak City	19	18. Iron Springs compared to Donjek and Platte Rivers	41
17. Structural cross sections	20	19. Depositional model	42
18. Overturned anticline at Mahogany Hollow	21		
19. Tertiary folds of northern Canyon Range	22	Shnabkaib Member of the Moenkopi Formation:	
20. Canyon Range allochthon subthrust surface	24	Depositional Environment and Stratigraphy near	
21. Geological map of Canyon Range area	26	Virgin, Washington County, Utah, by Ralph E.	
Depositional Environment of the Iron Springs For-		Lambert	47
mation, Gunlock, Utah, by Brad T Johnson	29	Abstract	47
Abstract	29	Introduction	47
Introduction	29	Location	48
General statement	29	Methods of study and nomenclature	48
Location	29	Field methods	48
Previous work	30	Laboratory methods	48
Methods	30	Nomenclature	48
Acknowledgments	30	Regional setting	48
Geologic setting	31	Previous work	49
Nomenclature	31	Acknowledgments	50
Age	31	Lithologies	50
Paleogeography	32	Clastic rocks	50
Geologic history	32	Ripple-laminated siltstone	50
Stratigraphy	33	Structureless or horizontally stratified siltstone	
Sandstone facies	33	and siliceous mudstone	50
Shale facies	35	Chemical precipitates	51
Conglomerate facies	35	Gypsum	51
Red siltstone facies	36	Bedded gypsum	51
Silty shale facies	36	Nodular gypsum	51
Dakota Conglomerate	36	Replacement or secondary gypsum	51
Measured sections	37	Laminated gypsum	51
Provenance	38	Limestone and dolomite	55
Depositional environment	39	Accessory minerals	55
Depositional model	40	Sedimentary structures	56
Summary	43	Ripple marks and bedding	56
References cited	43	Desiccation cracks	58
Appendix A	45	Soft-sediment deformation	58
Appendix B	46	Paleontology	58
Figures		Paleoenvironment	59
1. Index map	30	Paleoclimate	59
2. Detail of measured sections	31	Salinity	60
3. Tectonic setting	32	Water energy	60
4. Detail of tectonic setting	32	Lithologic associations	60
5. Generalized stratigraphic column	34	Direction of transgression	60
6. Laminated sandstone	34	Basin slope	61
7. Deformation in sandstone	34	Water depth	61
8. Cross-bedding	34	Sedimentary model	62
9. Histogram of sieve data from sandstone	35	Supratidal environment	63
10. Shale facies and deformation	35	Intertidal environment	63
11. Conglomerate facies	36	Subtidal environment	63
12. Red siltstone facies	36	Summary	63
13. Silty shale facies	37	References cited	64
14. Interbedded silty shale and sandstone	37	Figures	
15. Wavy bedding	37	1. Index map	48
16. Dakota conglomerate	38	2. Outcrop of Shnabkaib	49
17. Detailed stratigraphic column	39		

3. Stratigraphic sections	52, 53	Tertiary System	78
4. Photomicrograph: lenticular bedding	54	Diorite porphyry	78
5. Outcrop showing gypsum nodules	54	Shatter zone	79
6. Photomicrograph: secondary gypsum crystals ...	54	Quaternary System	79
7. Outcrop of laminated gypsum	54	Pediment gravels	79
8. Photomicrograph: algal laminated gypsum	55	Colluvium	80
9. Photomicrograph: peloidal oolitic wackestone .	56	Alluvium	80
10. Photomicrograph: oolitic grainstone with radial features	56	Landslide debris	80
11. Photomicrograph: intra-oolitic peloidal wacke- stone	56	Talus	80
12. Pyritic siltstone	56	Structural geology	80
13. Wavy lenticular bedding, mottled bedding, and possible ball-and-pillow structure	57	General statement	80
14. Outcrop showing mudcracks	59	History of laccolithic concepts in the Henry Mountains	80
15. Deformed bedding	59	Gilbert	80
16. Fossils	59	Hunt, Averitt, and Miller	81
17. Fence diagram showing lithologic percentages .	61	Intrusions	81
18. Depositional model	62	Stocks	81
Tables		Laccoliths	81
1. Comparison of ripple mark morphology with McKee	58	South Creek laccolith	81
2. Comparison of sections 6 and 8	61	Dugout Creek laccolith	83
Geology of the Mount Ellen Quadrangle, Henry Mountains, Garfield County, Utah, by Loren B. Morton	67	Bysmaliths	86
Abstract	67	Ragged Mountain bysmalith	86
Introduction	67	Pistol Ridge bysmalith	87
Location and accessibility	67	Other Intrusions	88
Methods	67	Laccolith west of Slate Flat	88
Acknowledgments	68	North Summit Ridge intrusions	88
Previous work	68	Structures that imply other intrusions at depth	89
Stratigraphy	68	Faults west of the Pistol Ridge bysmalith	89
General statement	68	Structures west of South Creek Ridge	89
Jurassic System	70	Subsurface information	90
Entrada Sandstone	70	Interpretations	90
Curtis Formation	70	Genesis of intrusions	90
Summerville Formation	70	Intrusive forms	91
Morrison Formation	72	Brittle deformation	91
Salt Wash Member	72	Confining pressures	91
Brushy Basin Member	73	Economic geology	92
Cretaceous System	73	Coal	92
Cedar Mountain Formation	73	Petroleum	92
Buckhorn Conglomerate Member	73	Metals	93
Upper unnamed shale member	74	Gravels	93
Dakota Sandstone	74	Water resources	93
Mancos Shale	75	Summary	93
Tununk Shale Member	75	References cited	94
Ferron Sandstone Member	75	Figures	
Blue Gate Shale Member	76	1. Index map	68
Muley Canyon Sandstone Member	77	2. Stratigraphic column	69
Masuk Shale Member	78	3. Bedrock geologic map of the Mount Ellen Quadrangle	71
		4. Entrada, Curtis, Summerville, and Salt Wash Members of the Morrison Formation	72
		5. Entrada, Curtis, Summerville Formations	72
		6. Salt Wash and Brushy Basin Members of the Morrison Formation and Buckhorn Con-	

glomerate Member of the Cedar Mountain Formation	73	Swasey Spring quarry	110
7. Buckhorn Conglomerate	74	Lithology	110
8. Ferron Sandstone and Blue Gate Shale	76	Graded bedding	110
9. Hummocky stratification of lower Ferron Sandstone	77	Soft-sediment folds	111
10. Quartzite inclusion in diorite porphyry	78	Low-angle truncations	111
11. Quaternary pediment gravels	79	Oriented fossils	111
12. Cross section D-D'	82	Fragmented organic debris	111
13. Low-angle reverse fault in front of South Creek-Bullfrog laccoliths	83	Tool marks, sole marks, and microscopic scouring	111
14. Closeup of overturned Ferron Sandstone	83	Depositional model	112
15. Cross section of B-B'	84	Paleoecology	113
16. Slate and slate breccia at Head of Bullfrog dike ..	84	Paleontology	113
17. Dugout Creek laccolith from Star Flat	85	Conclusion	113
18. Low-angle reverse fault in front of Dugout Creek laccolith	85	Acknowledgments	114
19. Dugout Creek laccolith	85	References cited	114
20. Cross section C-C'	86	Figures	
21. Cross section E-E'	87	1. Index map	97
22. Pistol Ridge bysmalith	88	2. Swasey Spring quarry	98
23. Rotated block of Salt Wash Member	89	3. Sponge Gully quarry	98
24. Perpendicular-type normal faults	90	4. House embayment	98
25. Ferron coal outcrop	92	5. House Range stratigraphic column	99
Depositional Environments and Paleocology of Two Quarry Sites in the Middle Cambrian Marjum and Wheeler Formations, House Range, Utah, by John C. Rogers	97	6. Lithologies, orientation, and abundance of organisms in the quarries	102
Abstract	97	7. Photomicrograph: shale in Marjum Fm. at Sponge Gully	103
Introduction	97	8. Photomicrograph: limestone in Marjum Fm. at Sponge Gully	103
Location	98	9. Photomicrograph: distribution grading	103
Swasey Spring site	98	10. Photomicrograph: graded peloids	103
Sponge Gully site	98	11. Soft-sediment fold	103
Methods of study	98	12. Trend of basin from movement of slumps	104
Previous work	98	13. Low-angle truncations	104
Stratigraphy	100	14. Large-scale gravity slide	104
Swasey Limestone	100	15. Small-scale gravity slide	104
Wheeler Shale	100	16. Oriented <i>Yuknessia</i>	105
Marjum Formation	100	17. Orientation of organisms at Sponge Gully	106
Weeks Limestone	100	18. Block diagram: depositional model	107
Sponge Gully quarry	100	19. Westward migration of carbonate bank	107
Lithology	101	20. Sponge Gully specks	108
Graded bedding	101	21. Tool marks	108
Soft-sediment folds	101	22. Sole marks	109
Low-angle truncations	101	23. Trace fossils	109
Oriented fossils	104	24. Photomicrograph: shale in Wheeler Shale at Swasey Spring	110
Fragmented organic debris	105	25. Photomicrograph: limestone in Wheeler Shale at Swasey Spring	110
Tool marks, sole marks, and microscopic scouring	105	26. Orientation of organisms at Swasey Spring	112
Depositional model	105	27. Swasey Spring specks	113
Paleoecology	109	Carbonate Petrology and Depositional Environments of Carbonate Buildups in the Devonian Guilmette Formation near White Horse Pass, Elko County, Nevada, by Stephen M. Smith	117
Paleontology	109	Abstract	117

Introduction	117	Sandy dolomite subfacies	137
Location	117	Lithofacies G	137
Methods and nomenclature	117	Conclusions	137
Previous work	118	References cited	138
Acknowledgments	119	Figures	
Geometry and carbonate petrology of lithofacies	119	1. Index map	118
Lithofacies A	120	2. Classification of carbonate rocks	118
Lithofacies B	120	3. Classification of stylolites	119
Alternating light and dark dolomite subfacies ..	120	4. Stratigraphic columns of measured	
Homogeneous dolomite subfacies	120	sections	122, 123, 124
Heterogeneous dolomite subfacies	120	5. Laminated character of lithofacies A	125
Lithofacies C	121	6. Alternating light and dark "spaghetti" dolomite	
Pelletal packstone/grainstone subfacies	121	subfacies	125
<i>Amphipora</i> packstone and wackestone		7. Closeup of alternating light and dark "spaghet-	
subfacies	121	ti" subfacies	125
Pelletal packstone and wackestone subfacies	121	8. "Spaghetti" dolomite	125
Skeletal packstone and wackestone subfacies ...	125	9. Stylolites separating light and dark dolomite	126
Peloidal wackestone and mudstone subfacies ...	128	10. Photomicrograph: xenotopic dolomite	126
Heterogeneous and homogeneous dolomites	128	11. Replaced stromatoporoids(?)	126
Lithofacies D	128	12. Photomicrograph: grainstone/packstone	126
Lithofacies E	128	13. Photomicrograph: <i>Amphipora</i> encrusted with	
Pelletal grainstone and packstone subfacies	129	algae	126
Skeletal pelletal packstone and wackestone		14. Scattered dolorhombs in wackestone fabric	126
subfacies	129	15. In situ bulbous stromatoporoids	127
Pelletal packstone and wackestone subfacies	130	16. Upside-down stromatoporoid biscuit	127
Lithofacies F	130	17. Tabular stromatoporoid	127
Peloidal-pelletal packstone subfacies	131	18. Photomicrograph: <i>Vermiporella</i>	127
Fenestral wackestone and mudstone subfacies ..	131	19. Photomicrograph: prismatic-wall-type calci-	
Sandy dolomite subfacies	131	sphere	127
Lithofacies G	132	20. Photomicrograph: spinose-wall-type calci-	
Paleontology	132	sphere	128
Diagenesis	133	21. Photomicrograph: fenestral fabric	128
Recrystallization	133	22. Prominent exposure of lithofacies E	129
Dolomitization	134	23. Oriented <i>Stringocephalus</i> in grainstone	130
Depositional environments of carbonate lithofacies	135	24. Photomicrograph: <i>Stringocephalus</i>	130
Lithofacies A	135	25. Photomicrograph: <i>Solenopora</i>	130
Lithofacies B	135	26. Felt Wash section	131
Lithofacies C	136	27. Photomicrograph: crinoid columnal	132
Pelletal packstone/grainstone subfacies	136	28. Nautiloid	132
<i>Amphipora</i> packstone and wackestone		29. Photomicrograph: ostracode clusters	132
subfacies	136	30. Photomicrograph: <i>Amphipora</i>	133
Pelletal packstone and wackestone subfacies	136	31. Photomicrograph: <i>Trupetostroma</i> (?)	133
Skeletal packstone and wackestone subfacies ...	136	32. Photomicrograph: <i>Hammatostroma</i> (?)	133
Peloidal wackestone and mudstone subfacies ...	136	33. Rugose corals	134
Heterogeneous and homogeneous dolomites	136	34. Photomicrograph: uniserial foraminifera	134
Lithofacies D	136	35. Photomicrograph: nodosinelled	134
Lithofacies E	136	36. Photomicrograph: endothyrid	134
Pelletal grainstone and packstone subfacies	136	37. Depositional model	138
Skeletal pelletal packstone and wackestone			
subfacies	137	Geology of the Steele Butte Quadrangle, Garfield	
Pelletal packstone and wackestone subfacies	137	County, Utah, by William W. Whitlock	141
Lithofacies F	137	Abstract	141
Peloidal-pelletal packstone subfacies	137	Introduction	141
Fenestral wackestone and mudstone subfacies ..	137	Location and accessibility	141

Methods	141	Conglomerate Member of the Cedar Mountain Formation	145
Previous work	142	5. Exposure of Buckhorn Conglomerate and upper members of the Cedar Mountain Formation and Dakota Sandstone	146
Acknowledgments	142	6. Exposure of Tununk Shale Member of the Mancos Shale	147
Stratigraphy and sedimentation	142	7. Exposure of Ferron Sandstone and Tununk Shale Members of the Mancos Shale	147
General statement	142	8. Exposure of Blue Gate Shale and Muley Canyon Sandstone Members of the Mancos Shale	148
Jurassic System	142	9. Blue Gate Shale transitional facies	148
Entrada Sandstone	142	10. Stratigraphic column of Muley Canyon Sandstone	149
Curtis Formation	144	11. Exposure of Muley Canyon-1 unit	150
Summerville Formation	144	12. Exposure of Muley Canyon-2 unit	151
Morrison Formation	144	13. Diagram of coal sections	152, 153
Salt Wash Member	144	14. Exposure of Muley Canyon-3, Masuk Shale-1, Masuk Shale-2, Masuk Shale-3, Tarantula Mesa Sandstone	154
Brushy Basin Member	145	15. Exposure of Muley Canyon-3 cliffs	154
Cretaceous System	145	16. Fluvial channel in Muley Canyon-3 unit	155
Cedar Mountain Formation	145	17. Stratigraphic column of Masuk Shale	156
Buckhorn Conglomerate Member	145	18. Stratigraphic column of Tarantula Mesa Sandstone	157
Upper member	146	19. Cliffs of Tarantula Mesa-1 and Tarantula Mesa-2	158
Dakota Sandstone	146	20. Sandstone lenses in Tarantula Mesa Sandstone ..	158
Mancos Shale	146	21. Structural contour map and simplified geologic map	160
Tununk Shale Member	146	22. Coal isopach map and simplified geologic map .	162
Ferron Sandstone Member	147		
Blue Gate Shale Member	148	Petrography and Microfacies of the Devonian Guilmette Formation in the Pequoop Mountains, Elko County, Nevada, by Winston L. Williams	167
Muley Canyon Sandstone Member	148	Abstract	167
Masuk Shale Member	155	Introduction and location	167
Tarantula Mesa Sandstone	156	Acknowledgments	167
"Beds on Tarantula Mesa"	157	Previous work	168
Tertiary System	158	Methods	169
Diorite porphyry intrusions	158	Geologic setting	169
Quaternary System	158	Microlithofacies	169
Pediment gravel	158	Packstone	170
Alluvial terrace gravel	158	Uniform Packstone	170
Stream alluvium	159	Mixed Packstone	170
Eolian sand and loess	159	Wackestone	170
Colluvium	159	Uniform Muddy Wackestone	170
Structural geology	159	Mixed Wackestone	170
General statement	159	Sandstone	171
Henry Mountains structural basin	159	Stromatolitic Boundstone	172
Structures associated with intrusive bodies	159	Dolomite and Dolomitic Units	173
Toreva-block slides	159	Paleontology	174
Economic geology	159	Upper Devonian	174
Coal	159	Lower Mississippian	178
Petroleum	163		
Construction materials	163		
Water resources	163		
Summary	163		
References cited	164		
Figures			
1. Index map	142		
2. General stratigraphic column	143		
3. Exposure of Entrada Sandstone, Curtis Formation, Summerville Formation, and Salt Wash Member of the Morrison Formation	144		
4. Exposure of Salt Wash and Brushy Basin Members of the Morrison Formation and Buckhorn			

Depositional model	178
Diagenesis	182
Economic significance	183
Conclusions	184
References cited	185
Figures	
1. Index map	168
2. Main buildup	169
3. Measured sections	in pocket
4. Photomicrograph: uniform sparry packstone	170
5. Photomicrograph: uniform muddy packstone ...	171
6. Photomicrograph: mixed sparry packstone	171
7. Photomicrograph: mixed muddy packstone	172
8. Photomicrograph: dolomitic uniform muddy wackestone	172
9. Photomicrograph: mixed sparry wackestone	173
10. Photomicrograph: mixed muddy wackestone	173
11a. Photomicrograph: cross-bedded sand unit	174
11b. Cross-bedded sand unit	174
12. Photomicrograph: stromatolitic boundstone (algal mat)	175
13. Photomicrograph: "correlation" dolomite unit .	175
14a. Photomicrograph: <i>Stromatopora cygnea</i>	176
14b. Photomicrograph: <i>Talaestroma steleforme</i>	176
14c. Photomicrograph: ? <i>Trupetostroma</i> sp.	176
15. Photomicrograph: diastem within a stromatoporoid's coenostea	176
16a. Photomicrograph: calcareous alga ? <i>Stenophycus</i> sp.	177
16b. Photomicrograph: calcareous alga ? <i>Keega</i> sp. ...	177
16c. Photomicrograph: calcareous alga ? <i>Litanaia</i> sp.	177
16d. Photomicrograph: calcareous alga ? <i>Ortonella</i> sp.	177
16e. Photomicrograph: calcareous alga ? <i>Tharama</i> sp.	177
16f. Photomicrograph: calcareous alga of unknown genus	177
17. SEM photomicrographs: Kinderhookian conodonts from Joana Limestone	179
18. Flanking beds on mound	180
19. Unconformable contact between Guilmette Formation and Joana Limestone	181
20. Long intraclast with possible ghosted isopachous rim	182
21. Idealized depositional model of mound and surrounding shelf sediments	183
22. Strained calcite	184

A Geologic Analysis of a Part of Northeastern Utah Using ERTS Multispectral Imagery, by Robert Brigham Young

Abstract	187
Acknowledgments	187

Introduction	187
Objective	187
Location	187
Previous work	187
Methods of investigation	188
Geologic setting	188
General statement	188
Geologic history	190
Phase I	190
Phase II	190
Phase III	190
Phase IV	191
Phase V	191
Phase VI	192
Classification	192
General statement	192
Lineations	192
Lineation distribution	192
Introduction	192
Quadrant description	192
Northwest quadrant	192
Northeast quadrant	192
Southeast quadrant	192
Southwest quadrant	192
Uinta Megalineament	193
Description	193
Structure	194
Geophysics	194
Economics	194
Towanta Megalineament	194
Description	194
Structure	194
Geophysics	194
Economics	195
Strawberry Megalineament	197
Description	197
Structure	199
Geophysics	200
Economics	201
Badlands Cliffs and Book Cliffs Megalineaments ..	201
Badlands Cliffs Megalineament	201
Description	201
Structure	201
Geophysics	201
Economics	201
Book Cliffs Megalineament	201
Description	201
Structure	202
Geophysics	202
Economics	202
Uncompahgre-Raft River Megalineament	202
Description	202
Structure	202
Geophysics	202

Economics	203	Annular structures	207
Scofield Megalineament	203	General statement	207
Description	203	Summary	207
Structure	203	References cited	209
Geophysics	203	Figures	
Economics	203	1. Index map	188
Wasatch East Megalineament	203	2. Drainage map with geomorphic provinces	189
Description	203	3. ERTS Image 5544-16413	190
Structure	204	4. Lineation map	191
Geophysics	204	5. Megalineaments	193
Economics	204	6. Annular structures	195
Wasatch West Megalineament	204	7. Tectonic map	196
Description	204	8. Aeromagnetic map	197
Structure	204	9. Bouguer gravity map	198
Geophysics	204	10. Recorded seismic activity map	199
Economics	205	11. Economic geology map	200
Analysis	205	12. Orientation histogram	205
General statement	205	13. Intersection frequency contour map	206
Computer analysis	205	14. Lineation density contour map	208
Linear intersection frequency	205	Publications and maps of	
Linear density	207	the Department of Geology	213

Shnabkaib Member of the Moenkopi Formation: Depositional Environment and Stratigraphy near Virgin, Washington County, Utah *

RALPH E. LAMBERT

Chevron USA, Concord, California 94520

Thesis chairman: HAROLD J. BISSELL

ABSTRACT

The Shnabkaib Member of the Triassic Moenkopi Formation near Virgin, Utah, records a shallow, fluctuating transgression eastward and subsequent withdrawal of the sea across a very broad shelf. Shallow water, warm arid climate, and restricted circulation due to low relief and shoal areas combined to cause hypersaline waters and the formation of coastal sabkhas.

Subtidal and lagoonal sediments are represented by gray, burrowed, and slightly fossiliferous silty ooid-peloidal limestone, structureless or laminated mudstone or shales, and pyritic siltstone. Thick gypsum beds formed from the evaporation of restricted ponds in the lagoonal area.

Widespread flat algal mats grew near the high-water line of the intertidal zone and are now represented by the muddy cryptalgal laminated gypsum. Also, representative of intertidal sedimentation are light gray or greenish gray laminated siltstone, peloidal micrite, and pyritic argillaceous siltstone. Parallel and symmetrical ripple marks, flaser and lenticular bedding, small-scale graded bedding, and mudcracks help to identify intertidal deposition.

Layers of gypsum nodules and associated laminated and contorted bedding help identify the sabkha/supratidal environment. Moderate brown horizontally laminated siltstones and silty mudstones or shales, combined with disrupted bedding, mudcracks, cusp ripple marks, and a lack of fossils also represent the supratidal/floodplain environment.

The Shnabkaib is significant since it represents the last transgression of the Cordilleran sea from the miogeosyncline eastward onto the craton. Contributions of this study are several; to the writer's knowledge this study has (1) the most detailed stratigraphic sections and more sections of the Shnabkaib than any other study in southwest Utah; (2) first attempted correlation of different Shnabkaib sections; (3) first description of cryptalgal laminated gypsum in the Shnabkaib; and (4) the only detailed depositional environmental analysis of the Shnabkaib.

INTRODUCTION

The Shnabkaib Member is the second youngest of the six members of the Moenkopi Formation of Early and (?) Middle Triassic age in southwest Utah. This member forms a conspicuous banded series of red and white siltstone, mudstone, gypsum, and minor amounts of sandstone, limestone and dolomite. Thick mats of stromatolites also accumulated during the time of deposition. The Shnabkaib Member represents a shallow, evaporitic marine transgression of the Cordilleran sea eastward across the Las Vegas-Wasatch hingeline onto the craton.

Excellent exposures of this member occur on the steep slopes which are protected by the overlying cliff-forming Shinarump Conglomerate Member of the Chinle Formation in the vicinity of Virgin, Washington County, Utah. These exposures afford a three-dimensional study of the stratigraphy, lithology, and sedimentary structures, thereby permitting an interpretation of the depositional environments of the sediments. Few detailed stratigraphic sections of the Shnabkaib have been published, nor has any correlation between sections or detailed paleoenvironmental analysis been found by this writer.

*A thesis submitted to the Department of Geology, Brigham Young University, in partial fulfillment of the requirements for the degree Master of Science, August 1983.

LOCATION

Eight sections were measured within a radius of 30 km of the town of Virgin (fig. 1). Sections 1 and 2 are on the southern flanks of Hurricane Mesa (Pioneer Mesa on some maps). Section 3 is to the west of North Creek road and 1 km past the Virgin Oil Field. Section 4 is on the south side of Gooseberry Mesa adjacent to Utah 59. Fair dirt roads pass near sections 5 and 7, which are on the flanks of Little Creek Mountain. Section 6 was measured near Utah 15 in Zion Park, and section 8 was measured a few kilometers south of the type section on the east flank of the Washington Dome, a part of the Virgin anticline. This last section is near an auto wrecker's lot.

METHODS OF STUDY AND NOMENCLATURE

Field Methods

A steel tape, Jacob's staff, Abney hand level, and Brunton compass were used to measure eight stratigraphic sections which total approximately 900 m. Different lithologies may be interbedded or very gradational, and hence many large units were divided by color. Lithology, composition, grain size (almost exclusively silt size or finer), color, sedimentary structures, and topographic expression were noted for each. Where possible, paleocurrent directions were measured and a search for fossils was undertaken. Approximately 100 hand samples were collected and analyzed in the laboratory. In each section studied, the gradational lithology between the Shnabkaib and the middle and upper red members makes selecting definite member boundaries and comparing overall thickness between different studies impractical. Stewart and others (1972, p. 19) state that there is a 30–100-m transition zone between the middle red and Shnabkaib members on the Colorado Plateau. The top of the Shnabkaib is

much easier to determine than the base. Therefore, it is difficult to accurately compare total thickness with sections from different researchers. Sections in this paper compare favorably with nearby sections by Gregory (1950), but section 8 is much thinner than the type section of Bassler and Reeside (1921).

Laboratory Methods

Hand samples were studied under a binocular microscope, and 90 thin sections were made and studied with a petrographic microscope. Composition, texture, cement, microsedimentary structures, and fossil content were studied. Alizarine Red S stain was used on some samples but mostly unsuccessfully because of the high percentage of clastic material and extremely fine grain or crystal size. Some rocks were dissolved in dilute HCl to determine the percentages and composition of the insoluble residue. Two samples of mudstone were crushed and sieved; particles smaller than 43 microns were subjected to X-ray diffraction analysis to determine composition. Energy dispersive X-ray analysis was used to help determine the composition of four samples.

Nomenclature

Color nomenclature of lithologic units follows the color chart published by the Geologic Society of America (1979). Grain-size nomenclature is the modified Wentworth Grade Scale of Dunbar and Rodgers (1957, p. 161). Terminology for bed and laminae thickness is that of Ingram (1954).

REGIONAL SETTING

The study area lies at or very near the Colorado Plateau and Basin and Range physiographic province boundary as well as near the Las Vegas-Wasatch hingeline. Geology of the region consists generally of essentially flat-lying Mesozoic sedimentary rocks and Cenozoic volcanic rocks. There are two major structures, the Hurricane fault and the Virgin anticline. Stratigraphically, the Moenkopi Formation rests disconformably on the Permian Kaibab Limestone and consists of six members in southwest Utah. These members are, in ascending order, Timpoweap Limestone (also termed Rock Canyon Conglomeratic Member), lower red, Virgin Limestone, middle red, Shnabkaib Shale, and upper red members. Overlying the Moenkopi is the Shinarump Conglomerate Member of the Triassic Chinle Formation. The Shinarump forms the resistant caprock of the mesas and the chocolate cliffs of the Grand Staircase of the Grand Canyon. In areas where the Shnabkaib is protected by the Shinarump, it forms steep slopes, but where unprotected it forms low rounded hills (fig. 2).

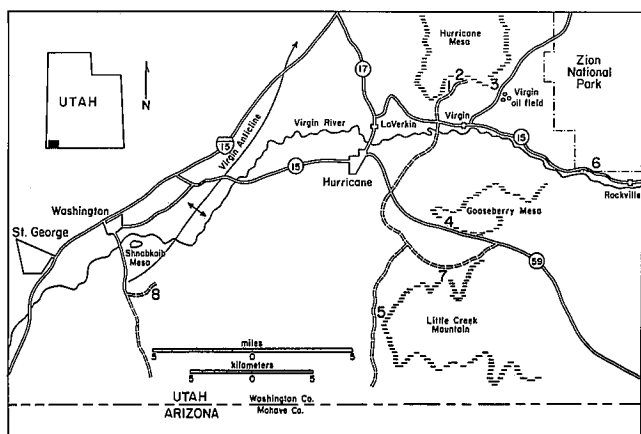


FIGURE 1.—Index map showing location and access of measured sections.

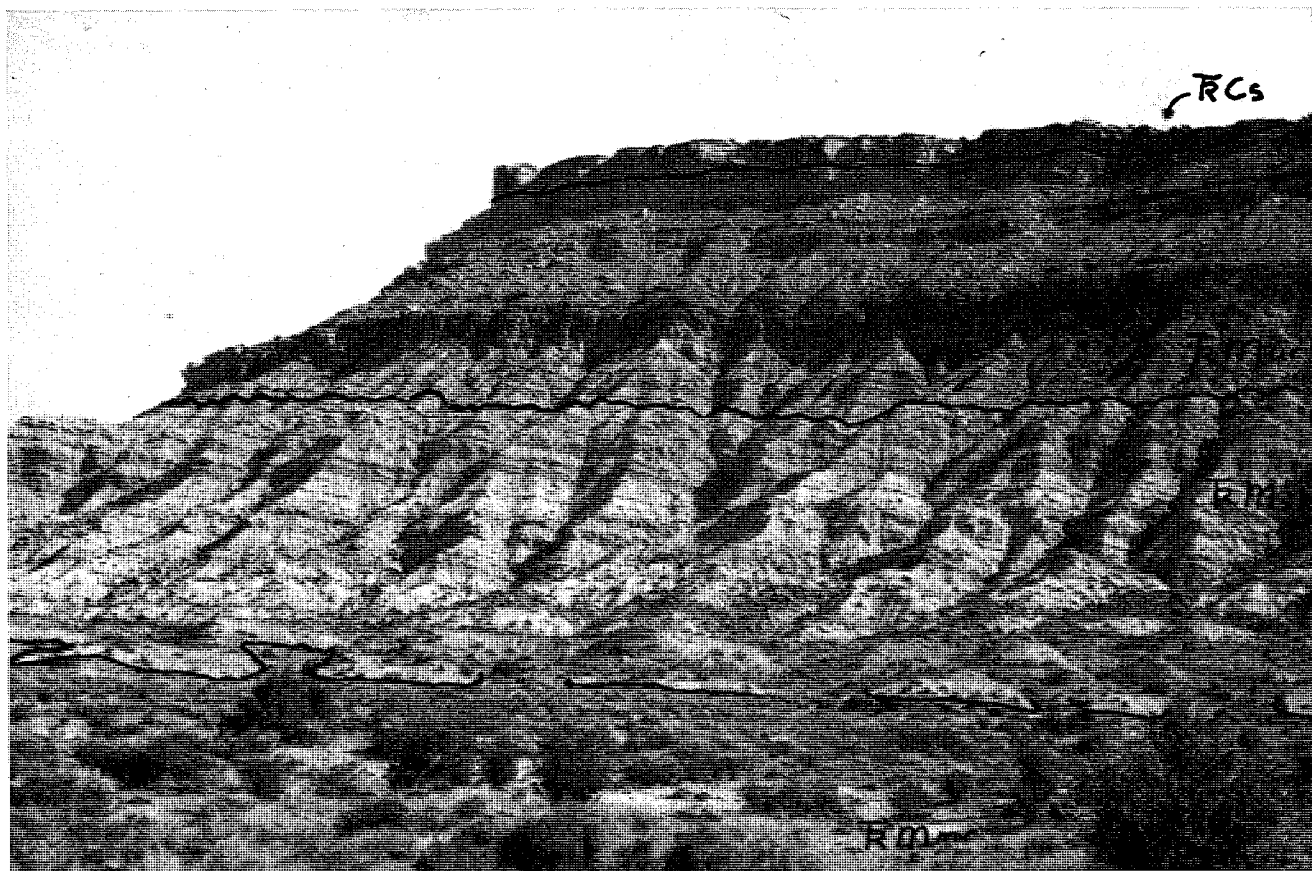


FIGURE 2.—Outcrop at section 4 showing approximate boundaries of Triassic Shinarump Conglomerate Member of the Chinle Formation, and the upper red, Shnabkaib, and middle red members of the Moenkopi Formation.

The Virgin Oil Field has historical interest since it is the oldest oil field in Utah, having been discovered in 1907, but economically it is unimportant (Gregory 1950, p. 190). What little oil is produced comes from shallow (180 m \pm) wells in the Timpoweap Limestone. Two shallow wells were drilled while fieldwork for this study was being undertaken but had not yet been placed in production when last visited in summer of 1981.

PREVIOUS WORK

Much work has been done on the Moenkopi Formation as a whole and especially on its limestone members, but very little detailed work has been published on the Shnabkaib Member. Ward (1901) named the Moenkopi Formation, and, from its type locality in the Grand Canyon east of Arizona, it was traced to southwest Utah by Huntington and Goldthwait (1904). Bassler and Reeside first used the name "Shnabkaib Shale Member" in 1921, but they actually proposed the name a year later (Reeside and Bassler 1922). The member was named for an isolated mesa 5 km southwest of the town of Washington on the west flank of the Virgin anticline. On the USGS (1954)

Hurricane, Utah, quadrangle topographic map, the mesa is called Shinob Kibe, whereas on their map, Bassler and Reeside (1921) spelled it Shnabkaib. Reeside and Bassler (1922) reported that the name *Shnabkaib* is probably the corruption of an old Indian name meaning *Coyote Mountain*, but Gregory (1950) reported that it is a corrupted Indian name meaning *Mountain of the Lord* and that the mesa has an interesting legend behind it.

The two most helpful papers that deal in part with the Shnabkaib are by McKee (1954) and Stewart and others (1972). These papers are helpful since each describes the stratigraphy, lithology, and depositional environments of the Moenkopi Formation. Poborski (1954) and Baldwin (1973) each offered good information on environmental interpretation based on the lithology and sedimentary structures of parts of the Moenkopi, but neither dealt with the Shnabkaib Member. Cadigan (1971) dealt with the petrology of the formation and discussed the tectonic history and source rock areas during Moenkopi time. Gregory (1950), Wilson (1965), and Bissell (1970) gave helpful general information of the area, age, tectonic and depositional history, petrology, and fossil life of the Moenkopi For-

mation. Only three detailed measured sections of the Shnabkaib in southwest Utah were found (Gregory 1950). No detailed Shnabkaib stratigraphic columns were found.

ACKNOWLEDGMENTS

I wish to thank my thesis adviser, Dr. Harold J. Bissell, for guidance and help. Thanks are also given to Drs. J. R. Bushman and M. S. Petersen for their work on my committee. To E. W. Christensen of Chevron USA go thanks for petrographic help. I wish to thank the Garrett and Kahle families of St. George for their free room and board during most of the fieldwork. Finally, thanks to friends, family, fellow students, and co-workers for encouragement and suggestions. This thesis was funded in part by the Quey C. Hebrew Memorial Award, for which I am grateful.

LITHOLOGIES

CLASTIC ROCKS

In the measured sections, clastic rocks make up approximately 55% to 70% of the total lithology. No pattern of percent increase in clastics was seen in the sections measured, but further eastward clastic content does increase, as noted by the writer. This eastward increase of clastics is also reported by Stewart and others (1972, p. 20) and can be explained by shallower water and an eastward source area. Most of the clastic rocks are calcareous (or dolomitic) and gypsiferous to some extent. Figure 3 illustrates the stratigraphic columns of the measured sections.

The main rock type of the Shnabkaib, comprising approximately 65% of the member, is quartz siltstone, with various admixtures of sand, clay, gypsum, and limestone or dolomite. The writer divides the siltstone into two general categories, (modified after Stewart and others 1972), which are the ripple-laminated siltstone and the structureless or parallel laminated siltstone. Colors of the siltstones follow the pattern of the member as a whole, namely moderate brown, medium to very light gray, yellowish gray, greenish gray, and pinkish gray. The grayish siltstones tend to have more gypsum and carbonate and frequently stand out in relief more than the brownish variety.

Ripple-Laminated Siltstone

Included in the ripple-laminated siltstones are the ripple-marked or cross-laminated sandstone and siltstone. Frequently quartzitic siltstones have gypsum or calcite as either matrix or cement. Very fine textured greenish mica is often visible, especially on some bedding planes in this siltstone group. Some plagioclase is occasionally seen, as well as some tiny lathlike high-birefringent crystals which

are most likely the hornblende that was mentioned by Stewart and others (1972, p. 61). Other rock fragments and some heavy minerals are also found. Throughout the member, the quartz grains are angular to subrounded and fairly well sorted. These rocks could be classified as low-rank graywacke siltstones.

When seen in plain view, the ripples are small parallel ripples. The ripples themselves will be discussed in the section on sedimentary structures. Stewart and others (1972, p. 52-53) remarked that ripple-marked sediments are commonly in close association with mudcracks, salt crystal casts, and raindrop impressions. In the sections measured for this study, no salt casts or raindrop marks were found, but in sections 3, 4, and 7, ripple marks were found closely associated with mudcracks. Frequently, the ripple-marked strata seem to be closely associated with gypsum or stromatolitic gypsum beds. Usually the ripple-marked siltstones are light in color though they do occur in the brown sediments.

Structureless or Horizontally Stratified Siltstone and Siliceous Mudstone

The writer believes that the structureless or horizontally stratified siltstones and mudstones are genetically related, since they are interbedded and have similar sedimentary features. Thus, these types of siltstone and mudstone are grouped together in this discussion. These lithologies are the most abundant in the Shnabkaib of the area studied. Some ripple marks are found in silty mudstones and form what Reineck and Singh (1975, p. 98) call lenticular bedding. Lenticular bedding is similar to flaser bedding except that mud, rather than silt, dominates because of lower energy and less silt input. Stratification mainly forms thin lamina (1-3 mm) but ranges from very thin to thick lamina, or structureless beds. Individual beds usually seem fairly persistent, but on a microscopic level the lamina may be seen to be discontinuous laterally. Some of these lamina are formed by stringers/layers of mud or coarser silt (fig. 4). Structureless siltstones tend to be finer grained and softer than siltstones that are ripple marked and often break into pieces less than 3 cm thick or, if massive, may weather into slightly rounded chunks.

Soft crumbly mudstone is fairly common in beds up to a few meters thick and frequently occurs in beds less than 1 m thick. The mudstone weathers to form recesses on slopes between more resistant lithologies. The mudstone is commonly moderate brown or greenish gray in color. These two colors of mudstone often occur adjacent to each other and have gradational contacts with one another. Sometimes there is a blob of mudstone of one color completely surrounded by mudstone of the other color. X-ray diffraction analyses were run on one mudstone (marl may be a better term) sample of each color from samples

1 m apart. They each contain quartz, dolomite, plagioclase, and a clay mineral. No reason for the color difference has been found. The mudstone appears to be structureless, but its crumbly nature would make it hard to preserve any internal structure. The mudstone falls apart when wet, and so it was impossible for the writer to make petrographically useful thin sections.

CHEMICAL PRECIPITATES

Gypsum

Gypsiferous rocks average 28% of the total lithology. There is no apparent pattern of increase or decrease in the percentage of gypsum among the eight sections, but the amount of massive pure gypsum tends to decrease eastward. In section 6 (the easternmost section) the thickest massive gypsum bed is only 20 cm thick as compared with up to 3 m in section 7. Stewart and others (1972, p. 20) reported a gradual thinning of the amount of gypsum as well as carbonates east of St. George. The writer confirmed this finding in field studies east of Zion National Park. Gypsum occurs as beds, ranging from several centimeters to several meters in thickness, layers of nodules, cement, and secondary crystals or crosscutting veins.

Bedded Gypsum. Beds of gypsum in the Shnabkaib are typically massive, internally structureless, finely crystalline, and white in color. The beds may be stained grayish pink, light brown, or pale green from slope wash or included muds. Gypsum beds range from several centimeters to 3 m thick, with 1–2-m beds common. Occasional thin layers of clear selenite are found. Selenite is often found as millimeter thick layers in the laminated gypsum. Massive gypsum beds, and in particular the laminated gypsum, are somewhat more resistant than most of the other rock types, thus forming erosional shoulders and ledges. Locally gypsum is underlain by a thin limestone (section 4—unit 5 and section 5—unit 2), but usually gypsum is underlain by horizontally laminated gypsiferous siltstone and silty mudstone. The beds tend to be fairly regular and continuous, though McKee (1954) reports lenticular gypsum. Gregory (1952, p. 61) reports that many beds extend for as much as a mile. The great majority of the crystalline gypsum beds occur in the light-colored sediments (light gray or yellowish gray). It is believed that many of these beds are too thick and regular to have formed from the coalescence of nodules. Also, there is an inverse relationship between how common nodules are in a section and gypsum bed thickness. No nodules are found in section 8 though it has the thickest beds of gypsum.

Nodular Gypsum. Gypsum nodules are finely crystalline and tend to occur along bedding planes and form both flat and rounded nodules up to 20 cm in size (fig. 5).

Kendall and Skipwith (1969, p. 858) and Friedman and Sanders (1978, p. 180) state that gypsum or anhydrite nodules grow in place from brines within the water table or capillary zone and above the high-water mark. Displaced sediments surrounding many nodules evince their growth in situ. When formed, nodules are usually anhydrite but upon hydration convert to gypsum (compare with modern examples, i.e., Reading 1979, p. 187).

Nodules are found in all sections except the westernmost (section 8) and are associated with both gray and brown horizontally laminated siltstones and mudstones. Nodules may have inclusions of greenish gray mud and small pyrite cubes and are often associated with massive beds of gypsum. Though nodules are secondary in origin, it is believed that they are helpful in determining environment since, as will be pointed out later, nodules are characteristic of a sabkha environment.

Replacement or Secondary Gypsum. Gypsum has apparently replaced some sediment, especially micrite and siliceous mud. Where well-developed crystals are found growing in mud, it is likely syngenetic since it would be difficult to form crystals and displace sediments after lithification (fig. 6). These sediments were still below the water table or at least within the capillary zone of the brine waters when the gypsum was introduced, since there must be some water circulation to concentrate the salts. There is much secondary gypsum which often occurs as veins of selenite or satin spar, up to 1 cm thick and found throughout the member. This gypsum occurs along bedding planes as crosscutting veins, and as large sheetlike deposits filling fractures. Secondary gypsum is essentially pure and often coarsely crystalline. Since this occurrence of gypsum is diagenetic, it is not seen as being important to the depositional environment.

Laminated Gypsum. Finely laminated gypsum beds are common in the Shnabkaib, comprising about 20% of the measured sections. Lamina of gypsum alternate with mud, wispy algal filaments, and minor amounts of dolomite or high Mg calcite (as indicated by energy dispersive X-ray analysis). Thin laminations occur in fairly clean gypsum, muddy or silty gypsum, and silty and/or gypsiferous mudstone. These beds are either grayish or brownish in color depending on the included mud. This lithology forms the most resistant of the thick units in the Shnabkaib. Ledges of algal (?) laminated gypsum are more common in the top half of the sections and are often as much as 5 m thick. Frequently, two or three of these ledges occur together, separated by 1–2 m of silty mudstone. The sediment is usually light in color, though much of it may have a brownish stain from slope wash.

Locally the gypsum in these beds occurs as millimeter-size lamina of selenite or clear gypsum, but more commonly it is a softer muddy gypsum. Laminated gypsum

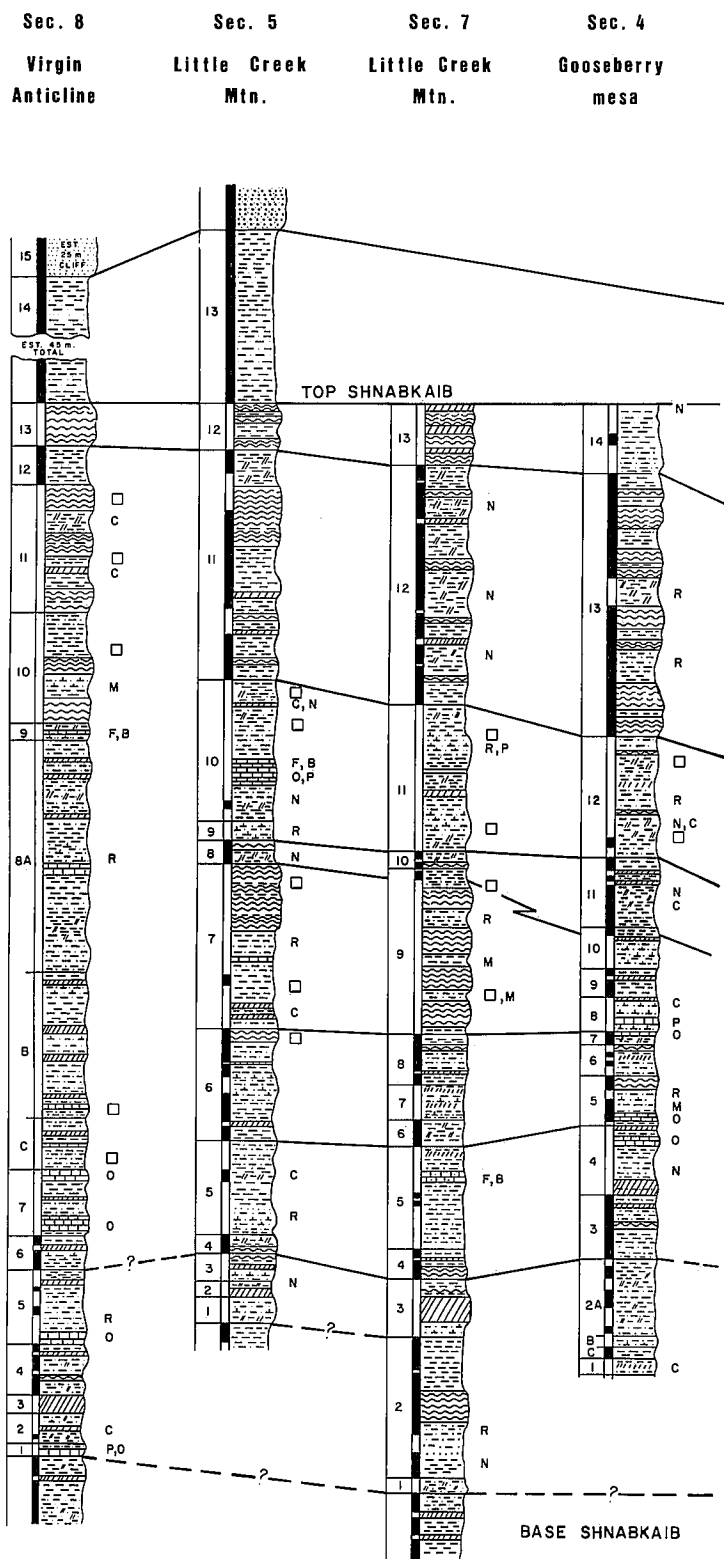
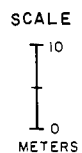


FIGURE 3.—Measured sections with suggested correlations. Correlations are based mainly on major color changes.



beds are not very calcareous, possibly because of replacement of carbonates by gypsum. Laminae in these extensive units are wavy, parallel, discontinuous, and clearly seen in weathered outcrop (fig. 7). Very fine to medium laminae are seen in thin section (fig. 8). Frequently the

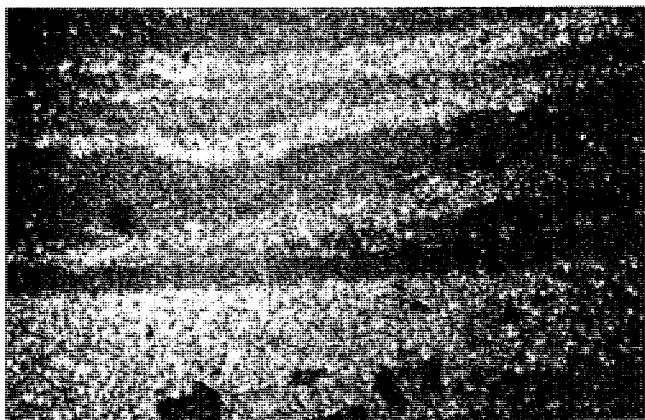


FIGURE 4.—Photomicrograph showing lenticular bedding with silt and mudstone, section 5, unit 5, crossed nicols; field of view is 8mm, X6.



FIGURE 5.—Layer of white gypsum nodules in medium light gray siltstone, immediately below a thin layer of grayish brown mudstone, section 4, unit 4.

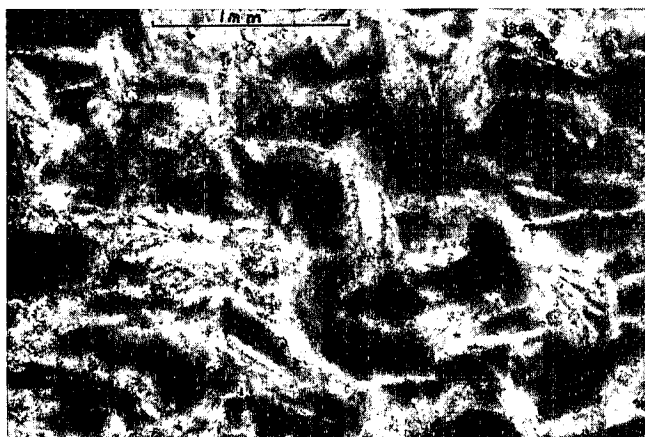


FIGURE 6.—Photomicrograph of secondary gypsum crystals in micrite, section 5, unit 5, crossed nicols, X15.

laminations are seen to be ripped up or distorted. This deformation is due to desiccation, current action, burrowing or grazing animals, growing algae, growing gypsum/anhydrite crystals, or the swelling due to the hydration of anhydrite to gypsum. A few mudcracks and burrows were found in associated sediments.

It is very difficult to distinguish mud lamina and cryptalgal filaments from each other. Indeed some of the so-called mud may be "algal dust." In any case mud and cryptalgal structures occur together, and it is believed that they formed in the same environment. Hereafter in this paper when algae are referred to, it should be understood that it is mostly laminated gypsum in outcrop, even though not all the lamina may be due to algae.

On the Abu Dhabi Coast in the Arabian Gulf, Park (1977, p. 493) has estimated that algal mats accrete at the rate of 2–5 mm per year. Gunatilaka (1975, p. 290) recorded 15 cm of mat growth in 12 weeks on the northwest coast of Sri Lanka. This second coastline has much more clastic input than the Abu Dhabi region. Park (1977, p. 493) states that after compaction and fluid loss the appar-

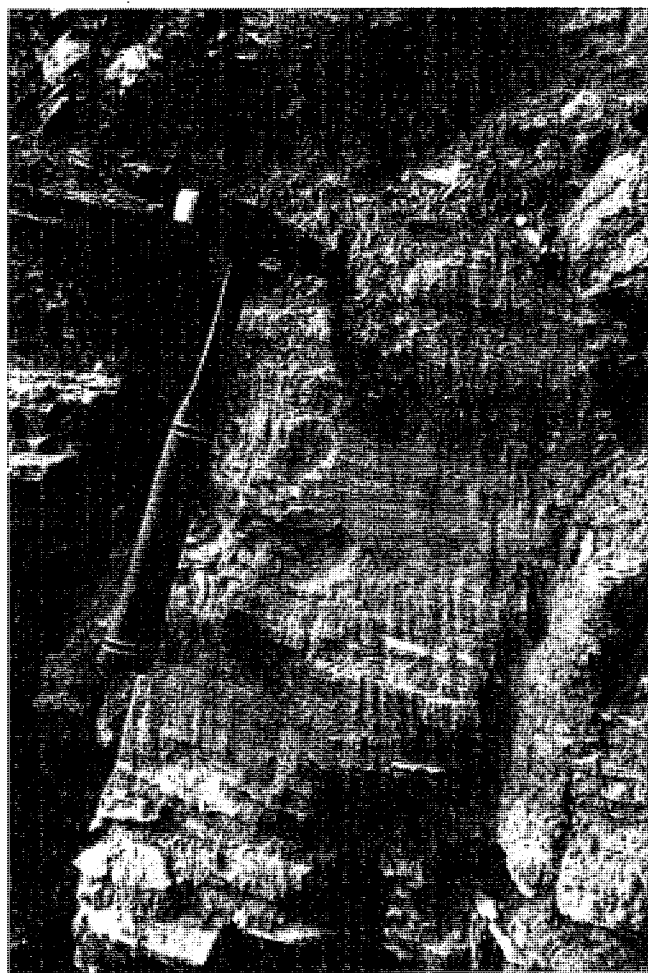


FIGURE 7.—Outcrop of soft laminated gypsum, section 2, unit 12.

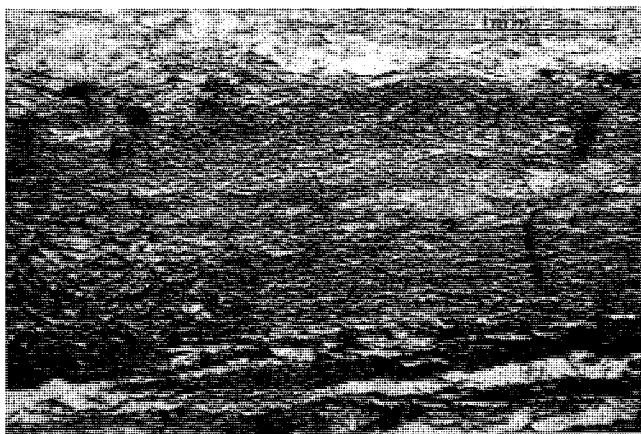


FIGURE 8.—Photomicrograph of very finely laminated gypsum with some disrupted cryptalgal lamina due to possible desiccation, section 2, unit 2, plain light, X15.

ent growth rate is 0.2 mm/year as estimated from 4,000-year-old algal mats, but he warns against trying to estimate time represented by the thickness of these sediments. It will suffice to say here that the Shnabkaib algal-laminated gypsum represents moderate periods of time in a similar environment of deposition. Gill (1977) showed planar stromatolites up to 6 m thick in his cross sections through the Silurian sabkha cycles of the Michigan Basin. No recent algal mats this thick are known to the writer.

Limestone and Dolomite

Cadigan (1971, p. 24) states that carbonates in the Shnabkaib near Hurricane are almost exclusively limestone as opposed to dolomite. In this study, both dolomite and calcite were identified in mudstone (as seen in two XRD analyses) and as cement in some siltstones. Energy dispersive X-ray analysis revealed dolomite or high Mg calcite in mud, oolitic rocks, (which also had calcite), and laminated gypsum. No rhombohedral or zoned dolomite crystals were seen in thin section. Carbonate beds are believed to be calcitic or high magnesium calcite from the reaction to acid and staining which was done. The microcrystalline and dispersed/impure nature of the carbonates made it difficult to distinguish between calcium and magnesium carbonate. Gregory (1950) reported that dolomite is common in one of three sections. Formation of gypsum lowers the calcium concentration of water, thus raising the Mg/Ca ratio so the precipitation of dolomite or high Mg calcite can be expected. Less dolomite was identified than expected, perhaps in part because of calcification. Calcite was found replacing small gypsum crystals, but calcification is not seen as a fully satisfactory answer. Activity of algae may tend to enhance formation of CaCO_3 (Friedman and Sanders 1978, p. 175), and much of the carbonate could have been replaced by gypsum.

Limestone beds always occur in the lower half of the measured sections and are light gray or yellowish gray in color. No "bed" of dolomite was noted. In the westernmost section (8) carbonates comprise about 7% of the sediments. From section 8 there is a fairly regular decrease eastward until in section 6 no carbonate beds are found. Overall, carbonate beds make up less than 4% of the eight sections.

Beds of limestone are typically associated with both subjacent and superjacent siltstone and mudstone. Sediments below the limestone are often less resistant than those above. There may be more gypsum or carbonate cement in the upper beds. Several occurrences of thin gypsum beds closely associated with limestone were noted. Once an overlying siltstone bed was noted to have current ripple marks, and in one place in section 1 the limestone was immediately overlying mudcracked mudstone.

Limestones are invariably silty (up to 15% by weight) and usually contain peloids and/or ooids (fig. 9). The ooids range in size from 0.15 to 0.8 mm in diameter with 0.4 mm being typical whereas the peloids are usually less than 0.1 mm in size (these measurements are made from thin sections). Oolites have sometimes been squashed and/or broken from compaction while still soft, forming spastoliths (fig. 10). These rocks would be classified as wackestone or packstone (Dunham 1962, p. 117). Diagenetic recrystallization is very common, as can be seen in figure 11 and from epitaxial rims visible in previous figures. Gypsum has replaced some of the preexisting micritic matrix, and thin selenite/gypsum veins were occasionally seen cutting an ooid. Thin siltstone stringers and small rip-up clasts were also seen in the limestones.

Reber (1951, p. 44) did not mention any limestone in the Shnabkaib of the northern Beaver Dam Mountains some 60 km to the west, probably because of the scale at which he measured his sections while mapping that area. On a brief field study some 55 km to the north near Cedar City, no limestone beds were noted by this writer, but 130 km to the north in the southern Pavant Range crystalline limestone beds are reported as being common in the Shnabkaib (Crosby 1959, p. 28; Bob Davis personal communication).

ACCESSORY MINERALS

Pyrite is the only accessory mineral readily seen in the field worthy of mention other than selenite/gypsum. It occurs as small cubes up to 1 mm, and is found only in the light colored (gray) sediments (fig. 12). Frequently, pyrite has been replaced by limonite which has stained the surrounding sediments a dusky red color. The resulting color contrast (dusky red on gray) facilitates recognition of pyritic zones.

Pyrite occurs in mud partings within gypsum, in gyp-

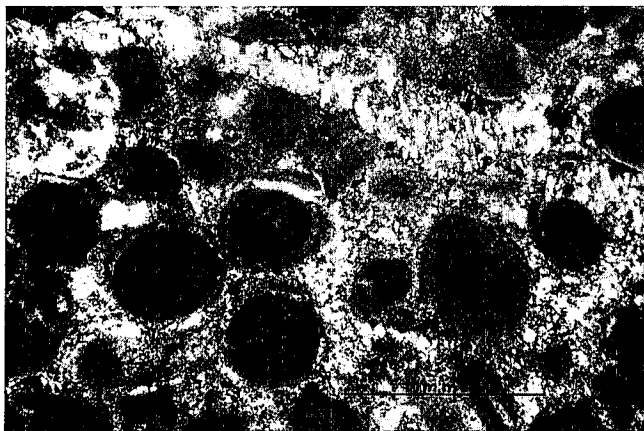


FIGURE 9.—Photomicrograph of a moderate brown sample of peloidal oolitic wackestone. Note that matrix has been replaced by gypsum, secondary fractures filled with satin spar gypsum, and epitaxial rims, section 8, unit 1, crossed nicols, X15.

siferous siltstones, in laminated gypsum, and at either the top or bottom of gypsum beds. It is stratigraphically controlled, being found on bedding planes, and is continuous for several meters. A general decrease in the amount and distribution of pyrite was noted from west to east, with no pyrite being observed in the easternmost section. In a roadcut along Interstate 15, a few kilometers south of St. George, pyrite is very common and forms cubes up to 5 mm in size. This roadcut is some 10 km east of section 8, where pyrite is also quite common but forms smaller cubes. The presence of pyrite in gray or greenish sediment is an indicator of reducing conditions at the time of formation, and hence the sediment was not subaerially exposed when deposited (Friedman and Sanders 1978, p. 525).

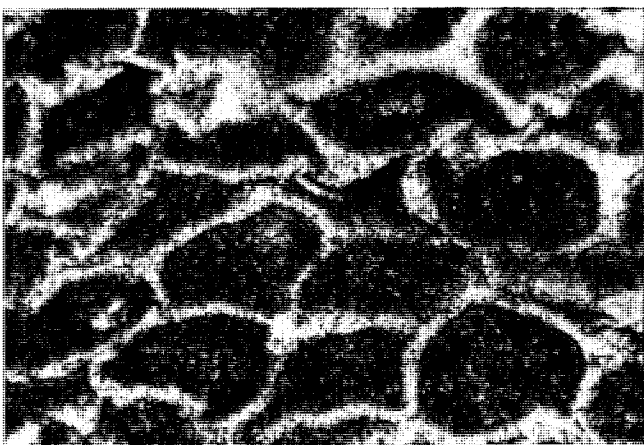


FIGURE 10.—Photomicrograph of oolitic grainstone showing radial fibrous structure and replacement by gypsum (?). Deformed and crushed oolites are called spastoliths and may indicate rapid deposition of overlying rocks; section 4, unit 5, (field of view is 1.3 mm), X37.8.

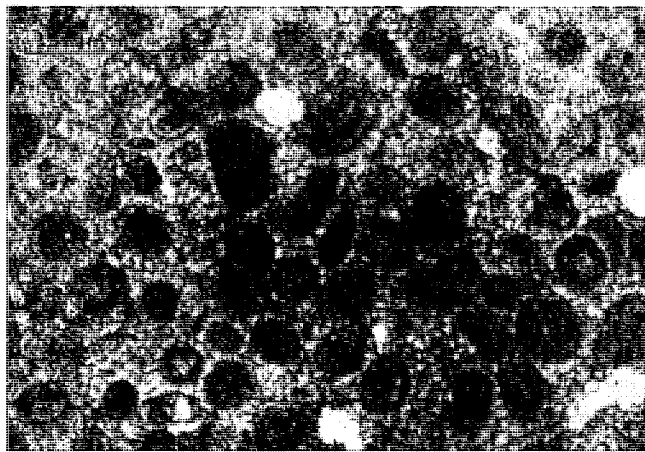


FIGURE 11.—Photomicrograph of intra-oolitic peloidal wackestone, mostly recrystallized calcite, section 5, unit 10, plain light, X15.

SEDIMENTARY STRUCTURES

In the section on lithology, several sedimentary structures were mentioned. Ripple marks and bedding were used as distinguishing characteristics in the siltstones. In addition, mudcracks, contorted bedding, scour marks, and small-scale ball-and-pillow structures were observed.

RIPPLE MARKS AND BEDDING

Commonly, individual beds are laminated or thinly bedded; rarely are beds more than a few centimeters thick. The main exceptions are the massive gypsum and layers of mudstone. The growth and diagenesis of gypsum would have destroyed any primary structure that may have occurred in the gypsum beds at the time of deposition.

Siltstones normally have even parallel beds which are continuous for several meters, though wavy lenticular



FIGURE 12.—A layer of small pyrite cubes on a muddy gypsiferous siltstone.

beds are found (fig. 13). Laminations are typically less than 3 mm thick and vary from even parallel to discontinuous, wavy, and nonparallel. In the shaly or muddy siltstones both flaser and lenticular bedding are common (fig. 4). As seen in figure 8, the laminae of the algal-laminated gypsum are very thin. Also of note are occasional interbedded and small-scale fining-upward sequences composed of coarse to fine silt.

Ripple-marked or cross-laminated sediments are fairly common and were found in one-fifth of the units measured. The ripple marks were less common than observed in some red bed members of the Moenkopi Formation in several localities. Because of the nonresistant nature of the Shnabkaib, few ripple-marked surfaces were found; cross-laminations, however, were more common. As a result, a meaningful statistical approach to transport direction, ripple-size, and morphology was essentially impossible. But what was seen compares very favorably with a sampling of 300 ripple marks in the Moenkopi by McKee (1954, p. 58) as seen in table 1.

Ripple marks and cross-lamination occur three times more frequently in the light-colored sediments than in the red or brown sediments, probably as a result of the gener-

ally more resistant nature of the light-colored rocks and as a function of primary deposition. The typical ripple mark in the Shnabkaib is a small asymmetrical parallel ripple which is thinly laminated and usually occurs in a thin to medium bed of siltstone. Variations include bifurcation of crests, some symmetrical/bimodal ripples, and some which show a climbing character. Interference ripples were also seen in two localities, one near section 3 and another just south of St. George. Of 13 transport directions recorded from ripple marks in the measured sections, the average direction was N 12° W. At only one locality was a ripple-marked surface of a few square meters exposed—in a streambed north of section 3. It consists of several layers of straight-crested, parallel ripples with the transport direction consistent on any one layer but ranging from N 45° E to N 30° E in the different layers. Interference ripples were also present in these light gray siltstones. Near the base of section 2 was found the only large-scale cross-bedding (about 30 cm long). It was in association with lensing siltstone beds. This cross-bedding and lensing appear to be due to local current channeling.

Reineck and Singh (1975, p. 23) reported that a ripple index (ratio of ripple length to amplitude) greater than 15

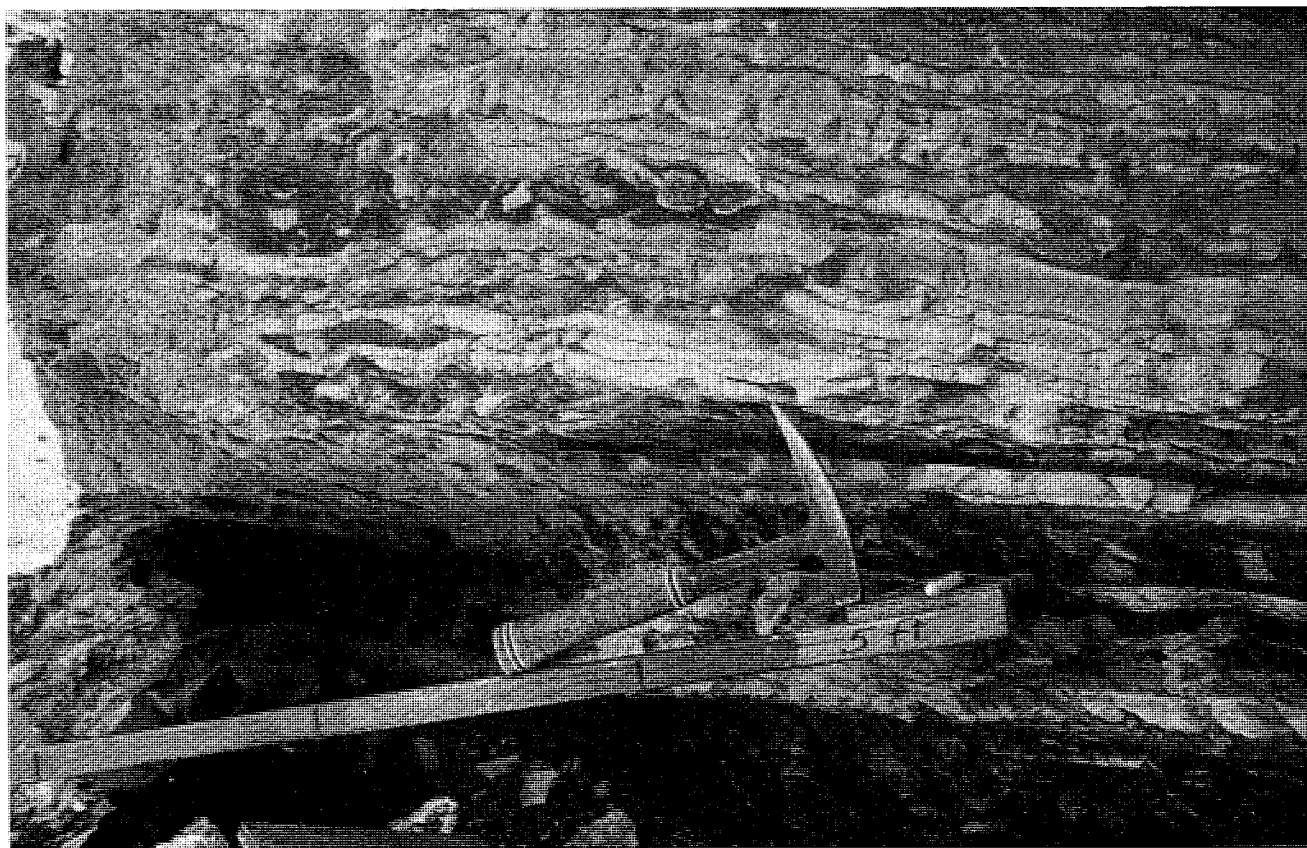


FIGURE 13.—Wavy lenticular bedding, mottled bedding, and possible ball and pillow structure in silt and mudstone; roadcut, section 2, unit 14.

Table 1. Comparison of Ripple Mark Morphology with McKee (1954)

		Range	Average	Mode
Ripple length	This study (13 readings)	18–35 mm	23 mm	25 mm
	McKee (300 readings)	13–76 mm*	25–38 mm**	25–38 mm
Ripple amplitude	This study	2–4 mm	3.2 mm	2 mm
	McKee	0.8–9.5 mm	3.2 mm	3.2 mm
Ripple index	This study	5–17	9	9
	McKee	5–15	9	8

*96% of McKee's readings fell within this range; he also reported 1% less than ½" (12.7 mm) long and 3% greater than 3" (76.2 mm) in length.

** McKee reported his lengths within ranges, thus no exact length is possible for comparison.

is formed only by wind or water currents and not waves. Various geologists report that an index of less than 15 is typical of formation by currents or waves and not wind (Reineck and Singh 1975, p. 46; and McKee 1954, p. 58). Indices of 8–15 are typically formed by currents whereas indices of 6–8 are most typical of waves (Reineck and Singh 1975, p. 45). Reineck and Singh (1975, p. 28) also reported that wave ripples have more regular crests which may bifurcate whereas current ripples are more irregular and bifurcation is absent. McKee (1954, p. 57) interpreted the most common ripple mark in his study, an asymmetrical parallel ripple mark with a ripple index of 9 and a length of 25 mm, as being formed by shallow-water currents. Interference ripples indicate both shallow currents and waves. The foregoing and association with other indicators of shallow water lead to the conclusion that ripple marks in the Shnabkaib were formed in shallow water by both currents and waves.

DESICCATION CRACKS

Desiccation cracks were seen in at least one area of each section except section 6. They could have been much more common than observed since good exposures are needed to see them, and it is difficult to find mudcracks preserved in the brittle mudstone which is typically covered by talus. Desiccation cracks seen were about evenly divided between the light- and red-colored sediments and were found in structureless or horizontally stratified siltstones and mudstones. In one instance, they were found directly on top of a bed of muddy gypsiferous stromatolite. The cracks typically are 1–2 cm across at the top, 1–5 cm deep, and 7–12 cm apart. These mudcracks are seen in plan view, in cross section, and as mud curls. Possible evidence of previous mud curls was seen in one unit with a mud pebble conglomerate. In section 2 some unusually large mudcracks are 5 cm ± wide, 12 cm ± deep, and some 15 cm apart (fig. 14).

SOFT-SEDIMENT DEFORMATION

Contorted bedding is common in the Shnabkaib and was frequently caused by growth of gypsum within the sediment (fig. 15). The gypsum nodules coalesce to form enterolithic structures. Much of the contortion is due to the hydration of anhydrite to gypsum and the in situ growth of anhydrite or gypsum crystals. Most of the convolute bedding is found in the light-colored sediments and is associated with gypsum. Tepee structures 3 cm ± high are fairly common in some gypsiferous laminated sediments.

In section 7, unit 5, a layer of yellowish gray calcareous mudballs 2 to 3 cm in size were found. A few wavy sub-millimeter black (organic?) streaks were seen in them. The mud balls were likely formed when a layer of mud or clay was broken up and became rounded due to the rolling action of small waves. Formation of such mud balls has been noted by the writer on the shores of Utah Lake, Utah. In section 2, unit 13, what appears to be cm-scale ball-and-pillow structure was noted (fig. 13). In a roadcut near St. George small-scale scour marks were found.

PALEONTOLOGY

Other than fossil algae remnants, little evidence of life has been found in the Shnabkaib. Probably because of high salinity and to diagenesis, the environment was apparently not conducive to a diverse fauna or to fossil preservation.

Gregory (1950, p. 63) listed fossils found in the Moenkopi in the Zion National Park region, and Stewart and others (1972, p. 67) reasoned by process of elimination that the "*Meekoceras micromphalus*" listed by Gregory was found in the Shnabkaib. If so, it was probably washed into the area and did not live there since the environment was not one believed capable of supporting ammonoid life. McKee (1954, p. 75) reported that Gregory collected a few poorly preserved and unidentified brachiopods, pe-

lecy-pods, and gastropods 20 to 50 m above the base of the Shnabkaib near section 3 of this paper. Though no fossils were found in section 3, I did find gastropod and pelecypod fragments in three other sections. The only other fossils found mentioned in the literature for this member are *Pentacrinus whitei* columnals in the Pavant Range 130 km to the north by Crosby (1959, p. 28) and Feast (1979, p. 30).

In this study, fossil remnants were found in one bed in sections 5, 7, and 8. These medium thick beds with fossils are invariably light-colored, silty, and muddy limestones with some short (up to 11 cm long) horizontal trails. In section 1 vertical burrows were found with no associated fossil fragments. These burrows are 2–3 cm deep and slightly curved at the base forming a *j*-like pattern. They occur in a yellowish gray muddy gypsiferous siltstone that also contains some algal filaments. All fossils are poorly preserved, lack internal structures, and are recrystallized or replaced. Gastropod fragments (1 cm in size) were found in section 5, small (1 cm) pelecypods (*Monotis* ?) and steinkerns (?) were found in sections 5, 7, and 8 (fig. 16).

Flat-lying algal mats, which were discussed briefly with laminated gypsum, were apparently very extensive at the time of deposition. The writer has yet to read of investigators mentioning algae in the Shnabkaib. A review of the literature on both ancient and modern algal mats showed that flat-lying algal mats (as opposed to blister, colloform, etc.) have the highest potential for preservation in the geologic record and are mainly composed of blue-green algae (Butler 1969, p. 73; Gunatilaka 1975, p. 292; Park 1977, p. 48; and Wilson 1975, p. 360).

The abundance of peloids seen in thin section is evidence of much more abundant burrowing or grazing life than otherwise thought from the few burrows and trails observed. Poor preservation of trails and burrows can be explained by crumbly mudstone and destructive nature of gypsum and algae both on and within the sediment. Gunatilaka (1975, p. 290), in his study of algal mats, observed

that, though cerithid gastropods were abundant on the mats, their trails were destroyed by sedimentation and algal growth.

PALEOENVIRONMENT

Near the town of Virgin, Utah, rocks of the Shnabkaib Member of the Moenkopi Formation represent sedimentation along the fluctuating coastline of a very shallow hypersaline sea. Sedimentation took place during a minor eastward transgression of the sea in an arid climate across a broad floodplain. The shallow water and low relief of the coast caused a low-energy seaway.

PALEOCLIMATE

During deposition, the climate was likely uniformly warm and arid. Evidence for such a climate is derived from lithology, postulated latitude, and comparison with modern analogues of this environment. Red beds and evaporites are usually indicators of warm, arid climates.



FIGURE 15.—Deformed bedding caused by the growth of a large translucent gypsum nodule, section 3, unit 3.



FIGURE 14.—Large mudcracks (?) extending from gypsiferous siltstone into mudstone, road level, section 2, unit 11.

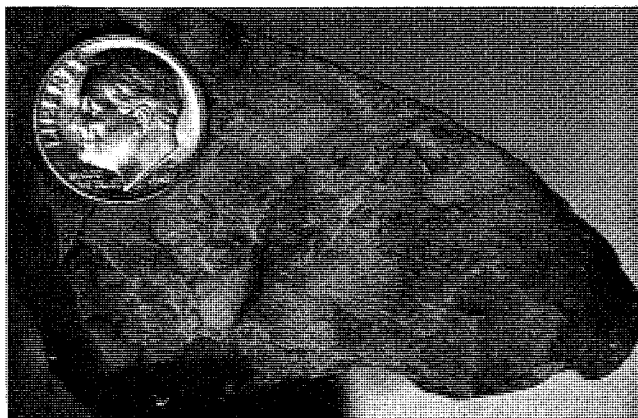


FIGURE 16.—Very silty limestone with best fossil found and some steinkerns (?); none of the original shell is preserved; section 8, unit 9.

Abundant gypsum is a clear indicator of net evaporation, and net evaporation is a function of both low precipitation and restricted circulation. Abundant algae and carbonate deposition are also enhanced by warm climates. Friedman and Sanders (1978, p. 180) state that nodular anhydrite is the signature of a sea-marginal sabkha in an arid climate.

Using paleogeographic and paleoclimatic maps of Dott and Batten (1971, p. 292, 345) it is estimated that southwest Utah was within 5° latitude of the equator and arid during deposition of the Shnabkaib. At such a latitude seasonal variations in temperature would have been minimal and warm weather the norm.

For comparison purposes it is postulated that the Abu Dhabi area of the Trucial Coast in the Persian Gulf is a modern analogue of the depositional environment of the Shnabkaib. It has been reported by Kinsman (1969, p. 838–39) that the average seawater temperature at the Trucial Coast is 29°C (84°F) and varies from 15°–40°C (59°–104°F). He also reports that for the formation and preservation of supratidal anhydrite a mean annual temperature greater than 22°C with seasonal fluctuations over 35°C is essential. Park (1977, p. 491) in his study of the same area reported that rainfall was less than 100 mm/yr and the air temperature varied from 15°–55°C (59°–131°F).

Another comparable arid evaporite coast is that found at the Ojo de Liebre Lagoons in Baja California. This series of lagoons lies 28° north latitude and average 20 mm of rain a year. Sediments there have a high percentage of clastics, halite, and gypsum but very little dolomite (Phleger 1969, p. 824).

SALINITY

Abundant gypsum is clear evidence of hypersaline conditions whereas the rare fossiliferous carbonates indicate more normal-marine salinities. Indirect evidence for hypersalinity is the lack of fossils throughout most of the rock record and the presence of thick algal mats. Friedman and Sanders (1978, p. 337) report that the cerithid gastropods which feed on the algae are less tolerant of high salinities than the algae. It is believed that in some modern areas algal mats are thin largely because of the voracious gastropods.

Scruton (1953, p. 2503) listed salinity ranges for precipitation of different minerals at typical densities as follows:

CaCO₃ precipitates from 72–199 ppm

CaSO₄ precipitates from 199–332 ppm

CaSO₄ & NaCl precipitate from 353–457 ppm

Park (1977, p. 487) reports salinities varying from 50–75 ppm in the algal mats at the Trucial Coast (normal seawater is 35 ppm). Gunatilaka (1975, p. 295) states that algae can tolerate salinities of 60 ppm without trouble, but

little more. Maximum salinities of 330 ppm have been found in sea-marginal pools associated with bedded gypsum at the Red Sea (Friedman 1978, p. 180). On the basis of these modern examples, it seems reasonable to expect that the salinities in the Shnabkaib sea and evaporating ponds would have ranged from about 40 to 350 ppm. Since no evidence was found for NaCl deposition, it is unlikely that salinities would have exceeded 350 ppm often or in large areas.

WATER ENERGY

Evidence indicates that at least the part of the Shnabkaib seaway studied was an area of low water energy. Structureless mudstone indicates deposition in standing bodies of water. Much of the fine sediment could have been blown in by the wind. Thin laterally continuous beds of fairly uniform thickness are often indicators of low-energy conditions as well as a gradual slope. A gradual slope would have dissipated wave energy over a large area and currents would have been nonexistent or very weak in the shallow waters. Other indicators of low energy include the very fine grained rocks, but such rocks can also be due to a distant and/or fine-grained source. There is evidence of areas of moderate energy with the clean oolitic carbonates which indicates enough energy to roll the particles back and forth and winnow away the fine sediment, but such a rock is rare here. More often the oolitic rocks are mixed with peloids and are only moderately well sorted. Lenticular and flaser bedding indicate alternate periods of currents and calm waters. These currents were likely tidal in origin. Cross-stratification from anything other than small ripples was observed only once and is found at the base of section 2. This occurrence of current cross-bedding could be from a small drainage channel off the tidal flats.

LITHOLOGIC ASSOCIATIONS

Lithologic associations indicate that the rocks of the Shnabkaib represent a shallow eastward transgression and subsequent withdrawal of the sea across an area of very low relief. The low slope caused wide variations in the strandline with minor changes in relative sea level or topography. Lack of rapid changes in the rock record is an indicator of distant or gentle broad tectonic activity at the time (a good review of the tectonics at that time is found in Cadigan 1971, p. 41–42). It is thought that numerous small fluctuations of the strandline are more likely due to migration, formation, and destruction of barrier bars or shoals than to tectonics.

Direction of Transgression

When compared to the enclosing middle red and upper red members, the Shnabkaib is clearly transgressive, but

just barely. In this area of Utah, the Moenkopi has three transgressive members: Timpoweap, Virgin Limestone, and the Shnabkaib; they are separated by three informal red-bed members. In each case, the transgression was from the west or northwest (Stewart and others 1972, p. 76; and McKee 1954, p. 78-79). The direction of transgression is also illustrated in figure 17 and in a comparison of sections 6 and 8, the most eastern and most western sections, respectively (table 2). Evidence of transgression and of shallow-water deposition discounts the possibility of a barred basin as a cause for deposition of evaporites in this area. Broad distribution of this member helps dismiss the possibility of gypsum deposition at the distal arm of a restricted sea (see isopach map of Stewart and others 1972).

Basin Slope

Intermixing of lithologies, scarcity of sharp lithologic boundaries, and the many color changes between gray and brown can be evidence for a slope of very low relief. Lateral continuity of beds also can indicate a gentle slope. A slight topographic variation such as a buildup of algae or an oolite ridge or barrier bar could cause ponding or a wide variation in the strandline. Wind-driven water could also affect the strandline and deposition substantially. Stewart and others (1972, p. 77) suggest that the depositional slope of the Moenkopi Formation may have been on the order of 1 foot per mile. At the Trucial Coast, the slope of the algae belt ranges from 1:1000 to 1:3000; also it is reported that algal mats do not develop if the slope is steeper than 1:1000 (Butler 1969, p. 73; Reading 1979, p. 182-86). Such a low slope could cause the intertidal zone to be several km wide with a tidal range of a few meters.

WATER DEPTH

As well as indicating energy, ooids can also indicate shallow water. It is reported that ooids form in water less than 6 m in depth (Greensmith 1978, p. 145). At Abu Dhabi ooids are found along barrier bars, in tidal deltas, and forming levees along tidal channels which are ex-

posed at low tide. At a depth of 2 m an abrupt change from pure oolite sands to mixed ooid-pellet sand takes place (Reading 1979, p. 179).

Blue-green algae can occur throughout the photic zone, which in normal seas may be as deep as 50 m. Schreiber (1981, p. 18) reasoned that, since hypersaline waters are often poorly oxygenated, there may be high organic residue in suspension, restricting light penetration to 10-20 cm or less. Evidence of poor oxygenation and high organics in the Shnabkaib may be the layers of pyrite. Pyrite is an indication of a reducing environment, which could be developed if decaying organic matter (algae) used up the available oxygen (Dunbar and Rodgers 1957, p. 212). At the Trucial Coast blue-green algae do not occur below 10 m water depth nor above the high-water mark (HWM), where it is destroyed by desiccation (Park 1977, p. 487).

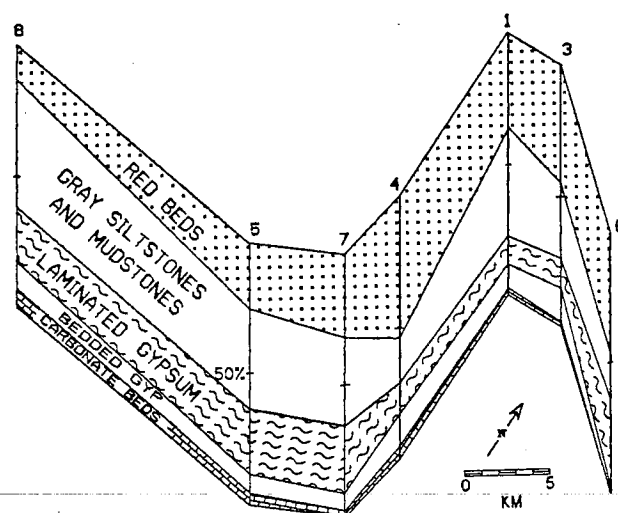


FIGURE 17.—Fence diagram depicting percentages of various lithologies. Section 2 is omitted since it is incomplete. Carbonate beds decrease and red beds increase from west to east, showing direction of transgression.

Table 2. Comparison of Sections 6 and 8

	Section 6 (easternmost)	Section 8 (westernmost)
1. thickness of section	69 m (least of the 8 sections)	123 m
2. amount of limestone	absent	most (of 8 sections)
3. fossils	absent	most (of 8 sections)
4. bedded gypsum	least	more
5. % red color	46% (green common also)	13% (least)
6. ripple marks	more common	rare
7. pyrite	absent	most common, largest crystals
8. gypsum nodules	common	absent

Algal mats are typical of the quiet water of the upper intertidal zone, though they do occur in other parts of the intertidal zone and up to lower supratidal, (Butler 1969, p. 73–74; Gunatilaka 1975, p. 292; Park 1977, p. 488; and Reading 1979, p. 181ff). The very shallow water postulated for the Shnabkaib did not allow the algae to build up as mounds or pillars, but only as flat mats.

Though gypsum per se does not indicate a particular water depth, it is more commonly found in very shallow waters. But as mentioned before, abundant gypsum nodules are formed in the capillary zone above the HWM. Other indicators of shallow water that are found are small rip-up clasts, mud-pebble conglomerate, climbing ripples, oscillation ripples, and mudcracks.

SEDIMENTARY MODEL

For the purposes of this paper environments represented in the Shnabkaib in the area studied will be divided into three basic subenvironments; namely, supratidal, intertidal, and subtidal (fig. 18). Much in these environments corresponds to standard carbonate facies #8 and

#9 of Wilson (1975, p. 350–60). He calls facies #8 “restricted circulation on marine platform” and facies #9 “platform evaporite facies.” Many recent papers have been written on evaporites, perhaps because of the petroleum potential in this environment (Kirkland and Evans 1981, Schreiber 1981). Authors on ancient evaporites frequently use Abu Dhabi as a modern example of a sea-marginal evaporitic environment.

On a broad shelf of such low relief as is postulated for this rock body, it is very difficult (and perhaps pointless at times) to differentiate between these environments. In particular, because of wind and slight tidal variations, the size of the intertidal zone would vary substantially in breadth. This would make a transition zone between the intertidal and supratidal zones and make the two indistinguishable from each other. Other difficulties with this member are the fine grain size and diagenesis. Fine grain/crystal size makes difficult mineral identification and interpretation of environment. Diagenesis can change the placement, mineralogy, and fabric of gypsum and result in the changing of nearby sedimentary structures. Di-

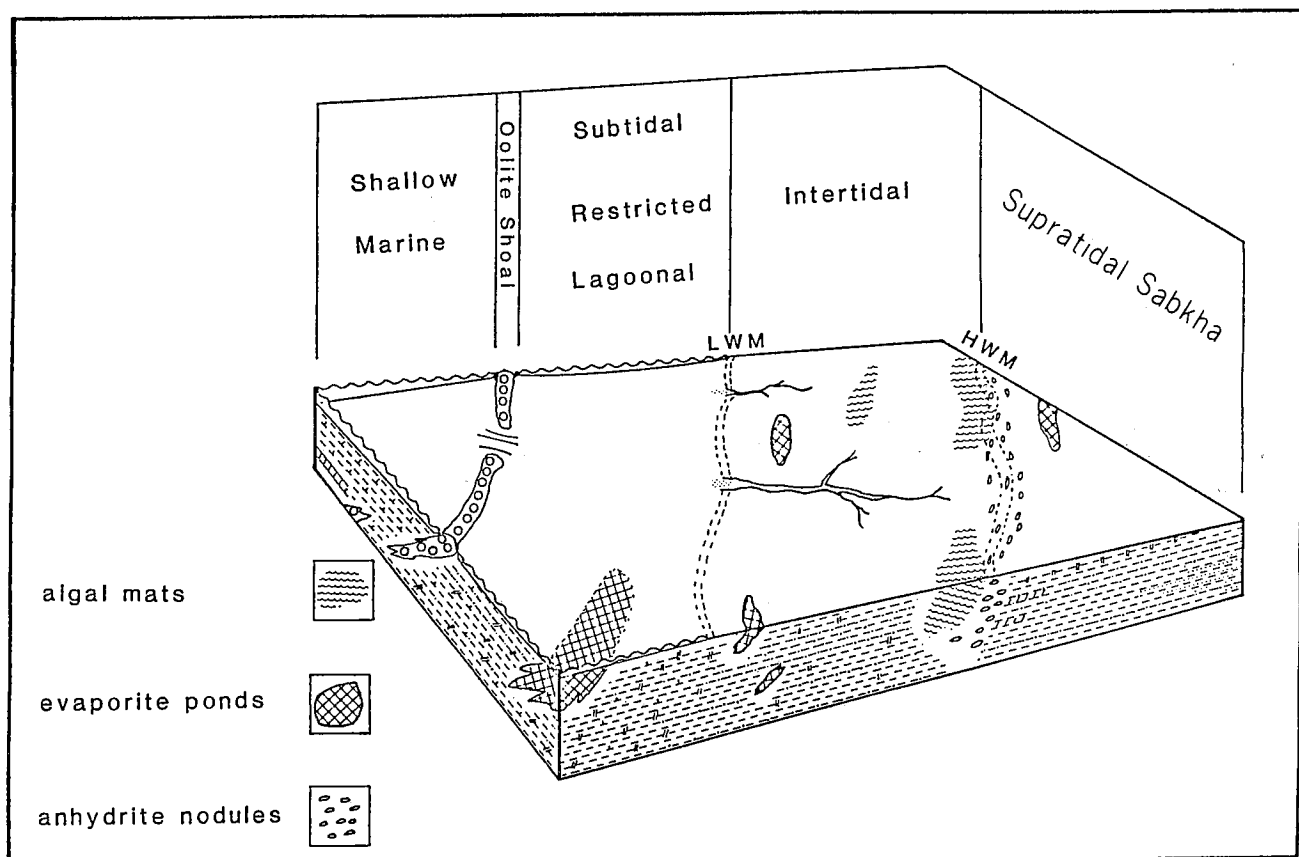


FIGURE 18.—Depositional model for the Shnabkaib member, showing wide intertidal areas with algal mats, gypsum nodules at high-water mark, and evaporitic ponds forming mainly in the restricted lagoonal area.

agenesis can also cause replacement of carbonates with each other or with gypsum, or it can cause changes in sediment color. Nevertheless the distinction will be attempted.

SUPRATIDAL ENVIRONMENT

Rocks deposited in a supratidal environment are those above the HWM but within the reach of storm or wind-driven water. Though perhaps not meeting this definition, any rocks from a coastal floodplain will be included in this section.

The presence of gypsum nodules seems to be one of the most readily identifiable lithologies/structures that is restricted to the supratidal coastal sabkha area, as was pointed out in the discussion on gypsum nodules. Nodules form above the HWM and within the water table or capillary zone. Nodules occur in both gray and brown horizontally laminated silts or muddy siltstones and often caused distortions in the sediments. Often the nodules were found near the gray/brown contact. Since the nodules grew within the sediment while the sediment was still soft, it is believed that the enclosing rocks were also formed in the supratidal or uppermost intertidal zone.

Another major indicator of supratidal deposition is the oxidized brownish sediments. But as pointed out by McKee (1954, p. 78) and Poborski (1954, p. 982-83), the color of primary reddish sediments deposited under tidal waters could have been preserved if the salinity had been sufficiently high to prevent the activity of sulphate-reducing bacteria. Though some red beds may be from tidal-flat areas, most are believed to have been deposited on a floodplain, especially when associated with cusp ripple marks, lithoclasts, and a scarcity of fossils. Association with intertidal deposits and similarities with the middle and upper red members help identify the red beds as terrestrial deposits. Other characteristics of supratidal deposits that are noted are gypsum, mudcracks, dolomitic sediments, and a lack of fossils. Some of the laminated gypsum is probably from this zone since discontinuous laminated sediments are characteristic of the supratidal environment (Lucia 1972, p. 170ff). But since most of the laminated gypsum is in the light-colored rocks, it is believed that most were formed in the intertidal zone.

INTERTIDAL ENVIRONMENT

Intertidal sediments are those which are deposited between normal high and low tides. This may be referred to as a tidal flat. As pointed out in the discussion on water depth, large flat-lying algal mats are most distinctive of the upper intertidal zone. As sediments are blown out or wash over the sticky algal mats, they are trapped. Mud, dolomite, gypsum, and pellets can be expected to be interlaminated with the algae. In the sections measured, dolo-

mite or high Mg calcite was identified with energy-dispersive X-ray analysis, but it did not seem to be common. Biota other than algae is rare in a hypersaline intertidal zone. However, some vertical burrowing organisms may occur (Heckel 1972, p. 244), but burrows are rare in the sections measured.

Gray or greenish siltstones, silty mudstones, gypsum, and pelletal lime muds are typical of an intertidal zone (Baldwin 1973, Reading 1979 and others) and are common in the Shnabkaib. This is especially true when combined with small parallel ripples, symmetrical ripples, flaser or lenticular bedding, and mudcracks. Also common to this environment and to the Shnabkaib are gray pyritic or limonitic silts and shales. Occasional lenticular cross-bedded siltstone and sandstone beds may indicate former channels that drained the tidal flats.

SUBTIDAL ENVIRONMENT

The subtidal environment is defined here as the areas in shallow water and below low tide, including lagoonal sediments. Shallow-marine rocks are represented by fossiliferous silty carbonates, oolitic carbonates, gray laminated shales (or mudstone), silty micrite, and pyritic silts and shales. Horizontal or U-shaped burrows and trails were occasionally seen and are more typical of shallow marine than of hypersaline intertidal or supratidal areas (Heckel 1972, p. 244, and others).

Sediments of restricted lagoons include gray laminated or structureless mudstones, siltstones, peloidal muds, and bedded gypsum (Lucia 1973, p. 162-64). The thickest gypsum beds are found in the westernmost sections where more water (and thus more salt) was available to evaporate to form thick gypsum beds. A great deal of water needed to evaporate to form such gypsum beds. Poborski (1954, p. 986) suggested that some of the bedded gypsum could be eroded from the underlying gypsiferous alpha member of the Permian Kaibab Limestone, but this writer does not know of any nearby place where the Kaibab Limestone was being substantially eroded during deposition of the Shnabkaib. Restricted lagoons could have been found in the intertidal zone, where they may have been periodically cut off completely from the sea. But the lagoons must have had periodic (at least) water recharge to have formed gypsum beds several meters thick.

SUMMARY

Rocks of the Shnabkaib Member near the town of Virgin, Utah, represent a shallow, fluctuating transgression from the west across a broad, gentle floodplain. Shallow water, a warm arid climate, and restricted circulation due to low relief and possibly, in part, to barrier bars combined to cause hypersaline waters and the formation of

coastal sabkhas. The end of Shnabkaib deposition occurred with the withdrawal of the sea to the west.

Subtidal and lagoonal sediments are represented by gray, burrowed, and fossiliferous silty ooid-peloidal limestones; structureless or laminated silty mudstones or shales; and pyritic siltstones. Gypsum beds formed from the evaporation of restricted lagoonal waters and hypersaline ponds. Extensive intertidal sedimentation is represented by thick accumulations of flat-lying muddy, cryptalgal laminated gypsum; light gray or greenish gray, laminated, muddy siltstones; peloidal micrites; and pyritic, argillaceous siltstones. Parallel and symmetrical ripple marks, flaser or lenticular bedding, small-scale graded bedding, and mudcracks help identify intertidal deposition. Layers of gypsum nodules and associated contorted bedding help to identify the supratidal environment. Also important in identifying the supratidal/sabkha and flood-plain environment are moderate brown, horizontally laminated siltstone and silty mudstone or shale. These lithologies are more diagnostic when combined with other features typical of a supratidal environment such as disrupted bedding, mudcracks, cusp ripple marks, and a lack of fossils.

The appendix for this paper, manuscript pages 1–20, is on file at the Department of Geology, Brigham Young University, where a copy may be obtained.

REFERENCES CITED

- Baldwin, E. J., 1973, The Moenkopi Formation of north-central Arizona—an interpretation of ancient environments based upon sedimentary structures and stratification types: *Journal of Sedimentary Petrology*, v. 43, no. 1, p. 92–106.
- Bassler, H., Reeside, J. B., Jr., 1921, Oil prospects in Washington County, Utah: U.S. Geological Survey Bulletin no. 726-C, p. 90–92.
- Bissell, H. J., 1970, Petrology and petrography of Lower Triassic marine carbonates of southern Nevada: *International Sedimentary Petrology Series*, v. 14, Leiden, Netherlands, 27p.
- Butler, G. P., 1969, Modern evaporite deposition and geochemistry of coexisting brines, the sabkha, Trucial Coast, Arabian Gulf: *Journal of Sedimentary Petrology*, v. 39, no. 1, p. 70–89.
- Cadigan, R. A., 1971, Petrology of the Triassic Moenkopi Formation and related strata in the Colorado Plateau region: U.S. Geological Survey Professional Paper 692, 70p.
- Crosby, G. W., 1959, Geology of the South Pavant Range, Millard and Sevier Counties, Utah: Brigham Young University Geology Studies, v. 6, no. 3, 59p.
- Dott, R. H., and Batten, R. L., 1971, *Evolution of the Earth*, 2nd ed: McGraw-Hill, New York, 489p.
- Dunbar, C. O., and Rodgers, J., 1957, *Principles of stratigraphy*: John Wiley and Sons, New York, 356p.
- Dunham, R. J., 1962, Classification of carbonate rocks according to depositional texture: In Ham, W. E. (ed.), *Classification of carbonate rocks, a symposium*: American Association of Petroleum Geologists Memoir 1, p. 108–21.
- Feast, C. E., 1979, The structural history of two klippen on the west flank of the Pavant Mountains, west central Utah: Master's thesis, University of Florida, Gainesville, 60p.
- Friedman, G. M., 1978, Depositional environments of evaporite deposits: In *Marine evaporites*: Society of Economic Paleontologists and Mineralogists, short course no. 4, Oklahoma City.
- Friedman, G. M., and Sanders, J. E., 1978, *Principles of sedimentology*: John Wiley and Sons, New York, 576p.
- Gill, D., 1977, Salina A-1 sabkha cycles and the Late Silurian paleogeography of the Michigan Basin: *Journal of Sedimentary Petrology*, v. 47, no. 3, p. 979–1017.
- Greensmith, J. T., 1978, *Petrology of the sedimentary rocks*, 6th ed: Unwin Brothers Ltd., London, 241p.
- Gregory, H. E., 1950, *Geology and geography of the Zion Park region, Utah and Arizona*: U.S. Geological Survey Professional Paper 220, 200p.
- Gunatilaka, A., 1975, Some aspects of the biology and sedimentology of laminated algal mats from Mannor Lagoon, north-west Ceylon: *Sedimentary Geology*, v. 14, p. 275–300.
- Heckel, P. H., 1972, Recognition of ancient shallow marine environments: In Rigby, J. K., and Hamblin, W. K. (eds.), *Recognition of ancient sedimentary environments*: Society of Economic Paleontologists and Mineralogists, Special Publication 16, p. 226–87.
- Huntington, E., and Goldthwait, J. W., 1904, The Hurricane fault in the Toquerville district, Utah: Harvard University Museum of Comparative Zoology Bulletin, v. 42, no. 5, p. 199–259.
- Ingram, R. L., 1954, Terminology for the thickness of stratification and parting units in sedimentary rocks: *Geological Society America Bulletin*, v. 65, p. 937–38.
- Kendall, C. G. St. C., and Skipwith, P. A. d'E., 1969, Holocene shallow-water carbonate and evaporite sediments of Khoral Bazam, Abu Dhabi, southwest Persian Gulf: *American Association of Petroleum Geologists Bulletin*, v. 53, no. 4, p. 841–69.
- Kinsman, D. J. J., 1969, Modes of formation, sedimentary associations, and diagnostic features of shallow-water and supratidal evaporites: *American Association of Petroleum Geologists Bulletin*, v. 53, no. 4, p. 830–40.
- Kirkland, D. W., and Evans, R., 1981, Source-rock potential of evaporitic environment: *American Association of Petroleum Geologists Bulletin*, v. 65, no. 2, p. 181–90.
- Lucia, F. J., 1972, Recognition of evaporite-carbonate shoreline sedimentation: In Rigby, J. K., and Hamblin, W. K. (eds.), *Recognition of ancient sedimentary environments*: Society of Economic Paleontologists and Mineralogists Special Publication 16, p. 160–92.
- McKee, E. D., 1954, Stratigraphy and history of the Moenkopi Formation: *Geological Society of America Memoir* 61, 133p.
- Park, R. K., 1977, The preservation potential of some recent stromatolites: *Sedimentology*, v. 24, p. 485–506.
- Phleger, F. B., 1969, A modern evaporite deposit in Mexico: *American Association of Petroleum Geologists Bulletin*, v. 53, no. 4, p. 824–29.
- Poborski, S. J., 1954, Virgin Formation (Triassic) of the St. George, Utah, area: *Geological Society of America Bulletin*, v. 65, p. 971–1006.
- Reading, H. G. (ed.), 1979, *Arid shorelines and evaporites*: In *Sedimentary environment and facies*: New York, Elsevier, p. 178–206.
- Reber, S. J., 1951, Stratigraphy and structure of the south-central and northern Beaver Dam Mountains, Washington County, Utah: Master's thesis, Brigham Young University, Provo, Utah.
- Reeside, J. B., Jr., and Bassler, H., 1922, Stratigraphic sections in southwestern Utah and northeastern Arizona: U.S. Geological Survey Professional Paper 129-D, p. 53–77.
- Reineck, H. E., and Singh, I. B., 1975, *Depositional sedimentary environments, with reference to terrigenous clastics*: Springer-Verlag, New York, 412p.
- Schreiber, B. C., 1981, Marine evaporites: Facies development and relation to hydrocarbons and mineral genesis, v. 2: Fall Education Conference, American Association of Petroleum Geologists, Calgary, Canada, 44p.

- Scruton, P. C., 1953, Deposition of evaporites: American Association of Petroleum Geologists Bulletin, v. 37, no. 11, p. 2498-2512.
- Stewart, J. H., Poole, F. G., and Wilson, R. F., 1972, Stratigraphy and origin of the Triassic Moenkopi Formation and related strata in the Colorado Plateau region, with a section of sedimentary petrology by R. A. Cadigan: U.S. Geological Survey Professional Paper 691, 195p.
- Ward, L. F., 1901, Geology of the Little Colorado Valley: American Journal of Science, 4th series, v. 12, p. 401-13.
- Wilson, J. L., 1975, Carbonate facies in geologic history: Springer-Verlag, New York, 470p.

